

# **Simulation of Breakthrough Curves for Dry Desulphurisation of Flue Gas in a Packed Bed Reactor**

*A Thesis Submitted  
in Partial Fulfilment of the Requirements  
for the Degree of  
Master of Technology  
by*

**SATISH KUMAR**

**Department of Civil Engineering  
Indian Institute of Technology Kanpur**

**May, 1995**

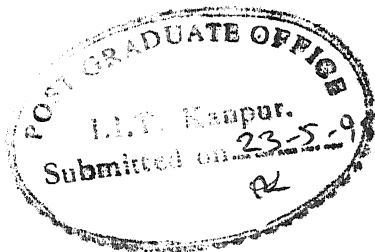
## CERTIFICATE

It is certified that the work contained in the thesis titled "**SIMULATION OF BREAKTHROUGH CURVES FOR DRY DESULPHURISATION OF FLUE GAS IN A PACKED BED REACTOR**", by *SATISH KUMAR*, has been carried out under my supervision and that this work has not been submitted elsewhere for a degree.

*K. Ghosh*  
22-5-95

Dr. D. K. Ghosh  
Department of Civil Engg.  
IIT, Kanpur.

May, 1995



22 APR 1996  
CENTRAL LIBRARY  
I. T., KANPUR  
No. A.121354

CE-1995-M-KUM-SIM



A121354

# ABSTRACT

An attempt has been made to predict the breakthrough curves for sulphur dioxide in a packed bed of solid reactants. An integrated software package has been developed to solve the involved differential equation and obtain the breakthrough curves using starbase graphics. Basic parameters required for predicting the breakthrough curves have been taken from the literature. Breakthrough curves for sulphur dioxide have been predicted using two solid reactants, namely, active sodium carbonate and calcined magnesium carbonate. For active sodium carbonate, breakthrough curves have been predicted for temperatures 150, 200, 250, 300, and 350 °C with an inlet sulphur dioxide concentration of 3500 ppm and for different inlet sulphur dioxide concentrations of 1500, 3500, 6000, and 18000 ppm keeping temperature constant at 200 °C. For calcined magnesium carbonate these have been predicted for temperatures 650, 750, and 850 °C with an inlet sulphur dioxide concentration of 9000 ppm and for concentrations 2000, 9000, and 22000 ppm keeping temperature constant at 750 °C. Model predicted breakthrough curves have been found to match fairly well with the experimental ones, except, in the case of those at higher temperatures (350 °C for active sodium carbonate and 850 °C for calcined magnesium carbonate). Departure may be attributed to the phenomenon of sintering at these temperatures.

*Dedicated  
to  
my parents*

# Acknowledgements

I take this opportunity to express my heartiest gratitude to Dr. D.K. Ghosh for his able guidance and supervision during my thesis work. I am indebted to him for his advices and help in all matters.

I am grateful to Dr. Malay Chaudhary, Dr. C. Venkobachar and Dr. Tare for shaping of my concepts in Environmental Engineering and for their love, inspisation and moral support.

I express my sincere and heartfelt thanks to my seniors Udaya Bhaskar, Alok Sinha and Rajesh Goyal for their help, guidance and cooperation.  
My heartfelt thanks to Induji for her active help and support.

I offer my thanks to Mansoor bhai, Anirbaan, Grasius, Javed, Ligy and Poornima for their help and cooperation.

I am thankful to all the staff members for their help and cooperation.

I remember Prasad, Rajesh, Apurb, Botke, P.K. Singh, K.K. Mishra, Arun Joshi and Diwakar whose company made my stay at I.I.T. Kanpur pleasant and memorable.

Thanks are due to 'Council of Scientific and Industrial Research' for financial assistance for carrying out this work.

I express my deep regards to my parents who have guided me all along the way of my life.

# Contents

<b>0</b>	<b>List of figures</b>	<b>ix</b>
<b>0</b>	<b>List of tables</b>	<b>xi</b>
<b>0</b>	<b>Nomenclature</b>	<b>xiii</b>
<b>1</b>	<b>Introduction</b>	<b>1</b>
<b>2</b>	<b>Background Information</b>	<b>3</b>
2.1	Introduction . . . . .	3
2.2	Harmful Effects of Sulphur Dioxide . . . . .	3
2.3	Sources of sulphur dioxide . . . . .	4
2.4	Flue gas desulphurisation systems . . . . .	4
2.4.1	Wet scrubbing . . . . .	5
2.4.2	Wet/Dry scrubbing . . . . .	5

2.4.3	Dry scrubbing . . . . .	5
2.5	Advantages of dry control technologies . . . . .	6
2.6	Dry desulphurisation in a packed bed . . . . .	6
<b>3</b>	<b>Scope of the work</b>	<b>9</b>
<b>4</b>	<b>Sulphation of solid sorbents and the packed bed model</b>	<b>10</b>
4.1	Sulphation of active sodium carbonate . . . . .	10
4.2	Sulphation of calcined magnesium carbonate . . . . .	11
4.3	Packed bed model . . . . .	11
<b>5</b>	<b>Results and Discussion</b>	<b>14</b>
5.1	Salient features of the software package . . . . .	14
5.2	Sample simulations . . . . .	15
5.2.1	Simulations for different values of $\sigma$ ( $y_L^* = 1$ ) . . . . .	16
5.2.2	Simulations for different values of $y_L^*$ ( $\sigma = 1$ ) . . . . .	16
5.3	Comparison of predicted and experimental breakthrough curves for active sodium carbonate. . . . .	19
5.3.1	At different temperatures . . . . .	19
5.3.2	At different Concentrations . . . . .	19
5.4	Comparison of predicted and experimental breakthrough curves for calcined magnesium carbonate. . . . .	23



5.4.1	At different temperatures . . . . .	23
5.4.2	At different Concentrations . . . . .	24
<b>6</b>	<b>Conclusions and Suggestions for Future Work</b>	<b>27</b>
	<b>References</b>	<b>28</b>
	<b>Appendices</b>	
<b>A</b>	<b>Source Code of the Software Package</b>	<b>30</b>
<b>B</b>	<b>Sample Simulations</b>	<b>47</b>
<b>C</b>	<b>Data Used for Simulation</b>	<b>50</b>
C.1	Data for active sodium carbonate . . . . .	50
C.2	Data for calcined magnesium carbonate . . . . .	51
<b>D</b>	<b>Simulated and Experimental Results</b>	<b>53</b>
D.1	For sulphation of active sodium carbonate . . . . .	54
D.2	For sulphation of calcined magnesium carbonate . . . . .	60

# List of Figures

5.1	Predicted breakthrough curves for different values of dimensionless reaction modulus, $\sigma$ . . . . .	17
5.2	Predicted breakthrough curves for different values of dimensionless distance, $y_L^*$ . . . . .	18
5.3	Predicted breakthrough curves for sulphation of active sodium carbonate at different temperatures, ( $C_{A_i} = 3500 \text{ ppm}$ ) . . . . .	20
5.4	Breakthrough curve for sulphation of sodium carbonate at $150^\circ\text{C}$ . . . .	20
5.5	Breakthrough curve for sulphation of sodium carbonate at $200^\circ\text{C}$ . . . .	21
5.6	Breakthrough curve for sulphation of sodium carbonate at $250^\circ\text{C}$ . . . .	21
5.7	Breakthrough curve for sulphation of sodium carbonate at $300^\circ\text{C}$ . . . .	22
5.8	Breakthrough curve for sulphation of sodium carbonate at $350^\circ\text{C}$ . . . .	22
5.9	Breakthrough curves for sulphation of active sodium carbonate at different concentrations, ( $T = 200^\circ\text{C}$ ) . . . . .	23
5.10	Breakthrough curves for sulphation of calcined magnesium carbonate at different temperatures, ( $C_{A_i} = 9000 \text{ ppm}$ ) . . . . .	24

5.11 Breakthrough curves for sulphation of calcined magnesium carbonate at 650 °C. . . . .	25
5.12 Breakthrough curves for sulphation of calcined magnesium carbonate at 750 °C. . . . .	25
5.13 Breakthrough curves for sulphation of calcined magnesium carbonate at 850 °C. . . . .	26
5.14 Breakthrough curves for sulphation of calcined magnesium carbonate at different concentrations, ( $T = 750\text{ }^{\circ}\text{C}$ ) . . . . .	26

# List of Tables

B.1	Simulations for different assumed values of ' $\sigma$ ' ( $y_L^* = 1$ ) . . . . .	48
B.2	Simulations for different assumed values of ' $y_L^*$ ', ( $\sigma = 1$ ) . . . . .	49
C.1	Data related to the active $Na_2CO_3$ pellet . . . . .	51
C.2	Data related to the calcined $MgCO_3$ pellet . . . . .	52
D.1	Sulphation of active sodium carbonate at $T = 150^\circ C$ , ( $C_{A_i} = 3500ppm$ )	54
D.2	Sulphation of active sodium carbonate at $T = 200^\circ C$ , ( $C_{A_i} = 3500ppm$ )	55
D.3	Sulphation of active sodium carbonate at $T = 250^\circ C$ , ( $C_{A_i} = 3500ppm$ )	56
D.4	Sulphation of active sodium carbonate at $T = 300^\circ C$ , ( $C_{A_i} = 3500ppm$ )	57
D.5	Sulphation of active sodium carbonate at $T = 350^\circ C$ , ( $C_{A_i} = 3500ppm$ )	58
D.6	Sulphation of active sodium carbonate at different concns., ( $T = 200^\circ C$ )	59
D.7	Sulphation of calcined magnesium carbonate at $T = 650^\circ C$ , ( $C_{A_i} = 9000$ ppm) . . . . .	60
D.8	Sulphation of calcined magnesium carbonate at $T = 750^\circ C$ , ( $C_{A_i} = 9000$ ppm) . . . . .	61

D.9 Sulphation of calcined magnesium carbonate at $T = 850^{\circ}C$ , ( $C_{A_i} = 9000$ ppm) . . . . .	61
D.10 Sulphation at different concentrations ( $T = 750^{\circ}C$ ) . . . . .	62

# Nomenclature

$A$	reactant gas
$A'$	frequency factor
$A_g$	surface area of grains of solids, $m^2/g$
$A_p$	external surface area of a particle or a pellet, $cm^2$
$b$	stoichiometric coefficient
$C_A$	conc. of $SO_2$ changing with the depth of the bed, $gmol/cm^3$
$C_{A_i}$	conc. of $SO_2$ at the inlet, $gmol/cm^3$
$C_{A_o}$	conc. of $SO_2$ at the outlet, $gmol/cm^3$
$d_o$	density of the solid reactant, $g/cm^3$
$D_e$	effective diffusivity, $cm^2/s$
$E_a$	activation energy, $cal./mol$
$F_g$	shape factor for the grain
$F_p$	shape factor for the pellet or particle
$k$	intrinsic reaction rate constant, $cm/s$
$L$	length of the bed, $cm$
$R, R_o$	radius of the pellet or particle, $cm$
$r$	coefficient of correlation
$t$	time, $min$
$t^*$	dimensionless reaction time
$U$	velocity of the gas, $cm/s$
$V_g$	pore volume, $cm^3$
$V_p$	volume of a pellet or particle, $cm^3$
$X$	fractional conversion
$y$	distance along the flow, $cm$

$y_L^*$  dimensionless length of the bed,  $cm$

## Greek symbols

$\alpha$	a distributed parameter
$\beta$	a function of $X$ and $\sigma$
$\epsilon_p$	porosity of a pellet or particle
$\epsilon_v$	void fraction of the bed
$\omega$	fractional volume of reactive solids
$\rho_p$	molar density of the solid reactant, $gmol/cm^3$
$\psi$	dimensionless outlet concentration
$\sigma$	dimensionless reaction modulus

# Chapter 1

## Introduction

Sulphur dioxide is released into the atmosphere through various sources such as coal-fired power plants, sulphuric acid plants, petroleum refineries, metal ore smelters, etc., the major source being coal-fired power plants. Among the various methods for control of sulphur oxides emissions cleaning up of flue gases received maximum attention.

Prior to 1980, the removal of sulphur dioxide by absorption was usually carried out by wet scrubbing. Owing to a number of problems and disadvantages associated with wet scrubbing, attention has now shifted to dry scrubbing which minimises or eliminates scaling, corrosion and sludge handling problems associated with wet scrubbing and also eliminates both the reheating requirements and high-pressure drop conditions.

The increased interest in dry flue gas desulphurisation (FGD) processes has led to the need for evaluating various sorbents. Evaluation of various sorbents under various process conditions may be facilitated if their performance can be predicted theoretically, using an appropriate model. Things are much more simplified if aid is taken of computer through the development of a software package.

The design of packed bed reactor involving gas-solid reactions poses considerable challenge because of the difficulties in characterising the transport and reaction processes of such reactors in a realistic manner. Szekely et al.(1976) quoted that in many instances even the individual steps involved in the overall desulphurisation process in a packed bed reactor are quite complex and inadequately understood. So the task of



presenting a workable model seems to be a formidable undertaking . Indeed, the state of affairs precludes the development of an entirely general 'all purpose' model which incorporates all the phenomena involved.

In this work, a computer software has been developed to solve the equations representing the grain model given by Szekely et al.(1976) and that has been used to predict the performance of the two sorbents ,namely, active sodium carbonate and calcined magnesium carbonate under various process conditions. A comparison has also been made between the predicted and experimentally observed values.

# **Chapter 2**

## **Background Information**

### **2.1 Introduction**

Air pollution is woven throughout the fabric of our modern life. The major cause of all air pollution is combustion. Sulphur dioxide is one of the air pollutants produced due to the impurities present in the fuel. Recognition of sulphur dioxide as one of the pollutants is not a recent phenomenon. Episodes of severe sulphur dioxide pollution date back to several decades which led to efforts to control its emission.

### **2.2 Harmful Effects of Sulphur Dioxide**

Various animal species, including man, respond to sulphur dioxide by bronchoconstriction, which may be assessed in terms of a slight increase in airway resistance. Sulphuric acid produced due to the presence of humidity is a much more potent irritant to man than sulphur dioxide.

Different species and varieties of plants vary in their sensitivity to sulphur dioxide exposures. Alfalfa is the most sensitive. Entry through stomata causes injury to leaf and may lead to plant damage and loss of crop yield (Wark & Warner, 1981).

Sulphur compounds are responsible for major damage to materials. Sulphur oxides accelerate metal corrosion, cause the loss of tensile strength of nylon and cotton fabrics. Sulphurous or sulphuric acids are capable of attacking a wide variety of building materials including limestone, marble, roofing slabs and mortar. (Offen et. al., 1987).

Droplets of sulphuric acid mist formed by photochemical reactions between sulphur dioxide and other pollutants, contribute significantly to the reduction in visibility.

Sulphuric acid formed in the atmosphere return to the ground as sulphates by means of dry and wet deposition. Acid deposition has a considerable impact not only on surface waters, but also on soils and ground water, mobilising micro nutrients and heavy metals and thereby impoverishing the status of the soils and poisoning drinking water.

## 2.3 Sources of sulphur dioxide

The sources of the oxides of sulphur are natural as well as anthropogenic, the latter being of prime importance to a pollution control engineer. The natural sources contributing to sulphur dioxide pollution are forest fires, volcanic eruptions and conversion of hydrogen sulphide into sulphur dioxide in the atmosphere. The past records and data indicate that nearly three fourth of anthropogenic sulphur dioxide emissions originate from the combustion of fossil fuels (Wark and Warner, 1981). Sulphur is present in all natural mineral oils and coal with a composition varying from 0.1 to over 5 percent. Fuel combustion in stationary sources and industrial processes are principal contributors of sulphur dioxide from human activities. About 69% of man-made sulphur dioxide emissions in India are attributed to the thermal power generation during 1990-91. Transportation contributes little to the anthropogenic sulphur oxides in the atmosphere, because the sulphur in the gasoline is low.

## 2.4 Flue gas desulphurisation systems

Flue gas desulphurisation (FGD) is presently the most commonly used technology to comply with sulphur dioxide emission requirements. FGD processes may be grouped

according to two classifications (i) throwaway and regenerative and (ii) wet, wet/dry and dry.

In throwaway processes, as the waste product formed is discarded, fresh chemicals must be continually added. In regenerative processes, removal agent can be continually regenerated in a closed-loop fashion. Throwaway processes have been found to be cheaper and less complex but involve waste disposal problems. Regenerative processes have been commercially tested but have been found to be much costlier. Wet or dry processes are differentiated simply on the basis that whether the product formed is dry or wet.

### **2.4.1 Wet scrubbing**

In this, removal of sulphur dioxide is achieved through chemical absorption by an alkaline solution. Even though wet scrubbing technology has been commercially proven, corrosion, erosion, scaling, large water requirements and relatively higher costs are some of the problems and disadvantages associated with it.

### **2.4.2 Wet/Dry scrubbing**

In this technology water requirement is reduced to one half of that for wet scrubbing with a view to reduce the problems associated with the use of circulating alkaline water solutions. In this, water in the solution sprayed into the flue gas stream evaporates by the heat of flue gases resulting in dry waste.

### **2.4.3 Dry scrubbing**

Dry scrubbing processes carry spray drying philosophy one step further by eliminating water usage entirely. In dry scrubbing processes, a dry alkaline powder is injected directly into the flue gas stream. The alkaline particles react with sulphur dioxide while suspended in gas stream. Dry waste product from this reaction is, subsequently, collected in a particulate collection device and the clean flue gas is vented to the

atmosphere.

## 2.5 Advantages of dry control technologies

Although the reactivity of dry scrubbing agents will naturally be somewhat lower than the reactivity of wet sorbent solutions used in wet scrubbing, dry scrubbing offers following advantages :

(i) The absence of water results in the minimization or elimination of corrosion, erosion, plugging and scaling problems.

(ii) Dry scrubbing processes control sulphur dioxide and particulates in a single piece of equipment. The capital costs of the process are projected to be 30 to 50% less than those of wet scrubber or spray drying systems.

(iii) Dry scrubbing process eliminates both the reheating requirements and high pressure drop conditions.

## 2.6 Dry desulphurisation in a packed bed

Dry sulphur dioxide removal in a packed bed of solid reactant involves gas-solid reaction. Gaseous pollutant reacts with the solid reactant and ,thus, gets removed. A gas-solid reaction system may involve several intermediate steps. Typically, these intermediate steps involve the following :

### REACTION- DIFFUSION

(1) Gas phase mass transfer of the gaseous reactant from the bulk of the gas stream to the external surface of the solid particle.

(2) (i) Diffusion of the gaseous reactant through the pores of the solid matrix, which could consist of a mixture of solid reactants and products.

- (ii) Adsorption of the gaseous reactant on the surface of the solid matrix.
- (iii) Chemical reaction at the surface of the solid matrix.
- (iv) Desorption of the gaseous product from the surface of the solid matrix.
- (v) Diffusion of gaseous reaction product through the pores of the solid matrix.

(3) Gas phase mass transfer of the gaseous product from the external surface of the solid to the bulk of the gas stream.

### HEAT TRANSFER

(1) Convective heat transfer between the gas stream and the surface of the solid particle, and

(2) Conduction heat transfer within the solid reactant product matrix.

### STRUCTURAL CHANGES

The reaction and heat transfer processes could lead to structural changes, such as sintering or changes in the pore structure, which in turn could have a marked effect on the overall reaction rate.

The mass transfer step has been extensively studied and is perhaps the best understood. Pore diffusion is inherently much more complex than diffusion in liquids or gases and, as a consequence, is much less understood. Some of the complicating factors are immediately apparent :

1) The volume occupied by the solids is not available for diffusive transfer.

2) The actual diffusion path will not follow a straight line but will be quite tortuous, and the extent of this tortuosity will, necessarily, depend on the pore structure of the solids.

The structural changes that may accompany gas-solid reactions can be quite complex and may be in the form of sintering, swelling, softening and cracking. Sintering implies

the phenomenon by which a porous compact increases its density as a consequence of being held at an elevated temperature, below its melting point. While a great deal of useful work is being done on sintering, the development of the field has not yet reached the stage where these models can be applied directly to the modelling of gas-solid reactions in which structural changes are important (Szekely et al., 1976).

Large number of experimental investigations on the process development with various types of reactive solids have been reported. However, very few studies deal with modelling and simulation of performance of a solid sorbent for desulphurisation in a packed bed.

One of the common materials used for sulphur dioxide removal is lime in its various forms. Marrier and Dibles (1974) have reported some data on sulphation of calcium oxide and magnesium oxide. Kinetics of reaction of sulphur dioxide with calcined limestone has been studied by Borgwardt (1970) and that with calcium oxide has been studied by Borgwardt and Harvey (1972).

A structural model was developed by Hartman and Coughlin (1974) to correlate the data on the reaction of sulphur dioxide with porous limestone in excess air at high temperature. Pigford and Sliger (1973) analysed the data of Borgwardt (1970) on the absorption of sulphur dioxide with porous calcium oxide and interpreted the data in terms of two diffusion processes - diffusion of sulphur dioxide through the pores and that through a layer of solid reaction product, coupled with chemical reaction.

Hartman and Coughlin (1976) proposed a grain model incorporating the chemical reaction and diffusional resistances. Alvors and Svedberg (1988) have further included the presence of inert matter in the particles. Ghosh et al. (1989) did modelling and simulation for desulphurisation of flue gas using dolomite. Dam Johansen et al. (1991) presented a modified grain model for the reaction between limestone, sulphur dioxide and oxygen taking into account the diffusion and external mass transfer to the particle surface. Karlegard and Bjerle (1994) compared the experimental results for desulphurisation of synthesis gas using zinc ferrite in a packed bed reactor, with those simulated on the basis of unreacted core model.

# Chapter 3

## Scope of the work

Significance of modelling and simulation of performance of a solid sorbent for desulphurisation needs no emphasis in view of the need for evaluating various sorbents in the dry flue gas desulphurisation systems. It also, helps in developing a better understanding of the processes involved.

Present work aims at predicting breakthrough curves for sulphur dioxide in a packed bed reactor of solid sorbents with the following objectives :

(i) Developing a customized and interactive software package to solve the involved differential equation and obtain the breakthrough curves,

(ii) To obtain predicted breakthrough curves for sulphur dioxide using the two solid sorbents, namely, active sodium carbonate and calcined magnesium carbonate under varying conditions of temperature and inlet sulphur dioxide concentration using the software developed and taking the basic parameters pertaining to the system like, rate constant, effective diffusivity etc. required for prediction from the literature (Bhaskar, 1994) and

(iii) Comparison of predicted breakthrough curves with the experimental ones, available in the literature cited above.

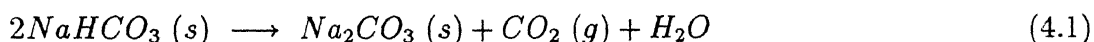


## Chapter 4

# Sulphation of solid sorbents and the packed bed model

### 4.1 Sulphation of active sodium carbonate

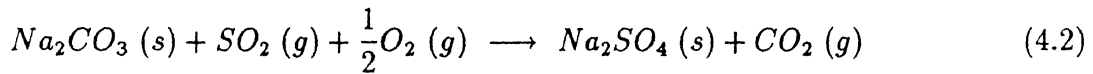
When sodium bicarbonate is exposed to flue gases at higher temperatures, thermal decomposition of the solid occurs producing the micrograin structured active sodium carbonate. Thermal decomposition of sodium bicarbonate above 115 °C is reasonably fast at atmospheric pressure yielding chemically active anhydrous sodium carbonate according to the equation (Bhaskar, 1994)



$\Delta G = 6.79 \text{ kcal.}$

The sodium carbonate formed according to above equation is known to have high surface area.

Active sodium carbonate reacts readily with sulphur dioxide and oxygen yielding sodium sulphate according to the reaction



$$\Delta G = -76.45 \text{ kcal.}$$

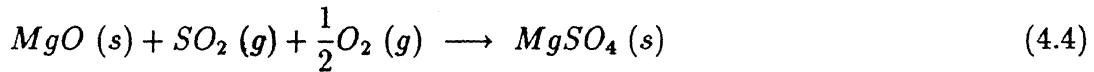
## 4.2 Sulphation of calcined magnesium carbonate

At higher temperatures magnesium carbonate decomposes according to the reaction



$$\Delta G = 11.55 \text{ kcal.}$$

In the presence of oxygen, the reaction of magnesium oxide with sulphur dioxide is given as



$$\Delta G = -71.95 \text{ kcal.}$$

## 4.3 Packed bed model

Using a shell balance (Szekely et al., 1976), variation of concentration of the pollutant, A, in an isothermal packed bed with plug flow has been shown as,

$$U \frac{\partial C_A}{\partial y} + (\epsilon_p + \epsilon_v) \frac{\partial C_A}{\partial t} + \frac{(1 - \epsilon_p)(1 - \epsilon_v)}{b} \omega \rho_B \frac{\partial X}{\partial t} = 0 \quad (4.5)$$

where,

$b$	stoichiometric coefficient
$C_A$	concentration of solute $A$ in the fluid phase
$S$	cross section of the bed
$t$	residence time
$U$	superficial velocity of fluid through the bed
$X$	fractional conversion of solid
$y$	distance along the length of the packed bed
$\rho_B$	molar density of reactant solid
$\epsilon_p$	porosity of the pellet
$\epsilon_v$	porosity of the bed
$\omega$	fractional volume of reactive solids in the bed

In dimensionless form the above equation reduces to (Ghosh et al.,1989)

$$\frac{\partial \psi}{\partial y^*} + \alpha \frac{\partial \psi}{\partial t^*} + \beta \psi = 0 \quad (4.6)$$

with the initial and boundary conditions

$$\psi(0, t^*) = 1 = f(t^*),$$

$$\psi(y^*, 0) = 0 = h(y^*) \quad (4.7)$$

where,

$$t^* = \left( \frac{bkC_{A_i}A_g}{\rho_b F_g V_g} \right) t \quad (4.8)$$

$$y^* = \frac{k}{U} \omega \left( \frac{A_g}{F_g V_g} \right) (1 - \epsilon_p)(1 - \epsilon) y \quad (4.9)$$

## CHAPTER 4. SULPHATION OF SOLID SORBENTS AND THE PACKED BED MODEL

$\alpha$  is a distributed parameter and is equal to

$$\frac{b(\epsilon_p + \epsilon_v)C_i}{\omega(1 - \epsilon_p)(1 - \epsilon_v)\rho_B} \quad (4.10)$$

$$\beta = \left[ \frac{1}{3}(1 - X)^{-2/3} + \sigma^2 \left( 2(1 - X)^{-1/3} - 2 \right) + (0.21 - 0.62X)(1 + \sigma^2) \exp \left( -0.9 \left( \ln \frac{\sigma}{1.08} \right)^2 \right) \right]^{-1} \quad (4.11)$$

$$\sigma = R_o \left[ \frac{(1 - \epsilon_p) A_g}{D_e V_g} \right]^{1/2} \quad (4.12)$$

The solution of Equation 4.6, through Laplace transformation has been obtained as follows,

$$\frac{C_{A_o}}{C_{A_i}} = \frac{dX}{dt^*} = \beta e^{-\beta y_L^*} \quad (4.13)$$

with the initial condition,

$$X = 0 \quad \text{when} \quad t = 0 \quad (4.14)$$

The above equation represents the packed bed model and its solution gives the variation of outlet concentration of gaseous reactant with time.

# Chapter 5

## Results and Discussion

### 5.1 Salient features of the software package

The software package developed is an interactive, integrated and customized one to develop the breakthrough curves for desulphurisation of flue gas in a packed bed reactor.

Some of its salient features are :

- It combines both the graphics as well as the problem solving features into one.
- It prompts the user for the input at various points of its execution.
- Input can be given either through the terminal or through input data-files.
- A number of sets of data can be given as input at a time and the solution is obtained in the form of output files. As many sets of data can be given as input as is required.
- It has the option for creating hardcopy of the output i.e the output can be printed on the plotter or the laser printer.

It creates \*.plt file to be directly sent to the plotter for printing and \*.bit file for the laser printer. The \*.bit file has to be first translated using the pcltrans command before sending the request to the laser printer.

Source code of the software developed is given in appendix A.

## 5.2 Sample simulations

Equations 4.13, 4.11, 4.12, 4.9 and 4.8 have been used for prediction of breakthrough curves. These are given here, again, for their easy reference for discussion.

Various basic parameters such as  $k$ , rate constant,  $D_e$ , effective diffusivity, etc. appearing in these equations are given in appendix C.

$$\psi = \frac{C_{Ao}}{C_{Ai}} = e^{-\beta y_L^*} \quad (5.1)$$

where,  $\psi$  is the dimensionless outlet concentration.

$$\beta = \left[ \frac{1}{3}(1-X)^{-2/3} + \sigma^2 \left( 2(1-X)^{-1/3} - 2 \right) + (0.21 - 0.62X)(1 + \sigma^2) \exp \left( -0.9 \left( \ln \frac{\sigma}{1.08} \right)^2 \right) \right]^{-1} \quad (5.2)$$

where,  $\beta$  is a function of  $X$ , fractional conversion and  $\sigma$ , dimensionless reaction modulus.

$$\sigma = R_o \left[ k \left( \frac{A_g}{V_g} \right) \frac{(1 - \epsilon_p)}{D_e} \right]^{\frac{1}{2}} \quad (5.3)$$

$$y_L^* = \frac{k}{U} \omega \left( \frac{A_g}{F_g V_g} \right) (1 - \epsilon_p) (1 - \epsilon_v) L \quad (5.4)$$

where,  $y_L^*$  is the dimensionless length of the reactor.

$$t^* = bk \frac{C_{Ai}}{\rho_B} \left( \frac{A_g}{F_g V_g} \right) t \quad (5.5)$$

### 5.2.1 Simulations for different values of $\sigma$ ( $y_L^* = 1$ )

Predicted breakthrough curves for different values of  $\sigma$  are given in Table B.1 and shown in Figure 5.1. It can be observed that breakthrough is delayed for lower values of  $\sigma$  and is quick for higher values.

From the expression for  $\sigma$  and  $y_L^*$ , it is clear that keeping  $y_L^*$  constant,  $\sigma$  can be made to vary with  $R_o$ , radius of the particle and  $D_e$ , effective diffusivity. Effects of  $R_o$  and  $D_e$  on breakthrough curves are discussed below. Explanations have been given both on the basis of concept as well as on the basis of mathematical equations representing the model.

#### Effect of $R_o$

Conceptually, for a given amount of solid reactant surface area available for reaction depends on the size of the particle. Surface area available being greater in the case of smaller particles and smaller in case of bigger particles. Hence, breakthrough will be delayed in the case of small particles and quick in the case of bigger particles.

From the equations given in the preceeding section, it is clear that for large  $R_o$ ,  $\sigma$  is large and hence  $\beta$  is small.  $C_{A_o} / C_{A_i}$  would be greater for small value of  $\beta$ . Hence, breakthrough would be quick in case of big particles and vice-versa.

#### Effect of $D_e$

Greater the effective diffusivity, more would be the access for the gas to the solid reactant and ,hence, more delayed would be the breakthrough curve. Reverse is the case for small effective diffusivity.

Greater the value of  $D_e$ , smaller the value of  $\sigma$  and ,hence, smaller the outlet concentration which means a delayed breakthrough curve.

### 5.2.2 Simulations for different values of $y_L^*$ ( $\sigma = 1$ )

Some predicted breakthrough curves for different values of  $y_L^*$  are given in Table B.2 and shown in Figure 5.2. It is observed that breakthrough is more and more delayed with increasing  $y_L^*$ .

From the expressions for  $\sigma$  and  $y_L^*$ , it is clear that while keeping  $\sigma$  constant,  $y_L^*$  can be made to vary with  $L / U$ , residence time,  $\omega$ , fractional volume of reactant solid, and  $\epsilon_v$ , void fraction.

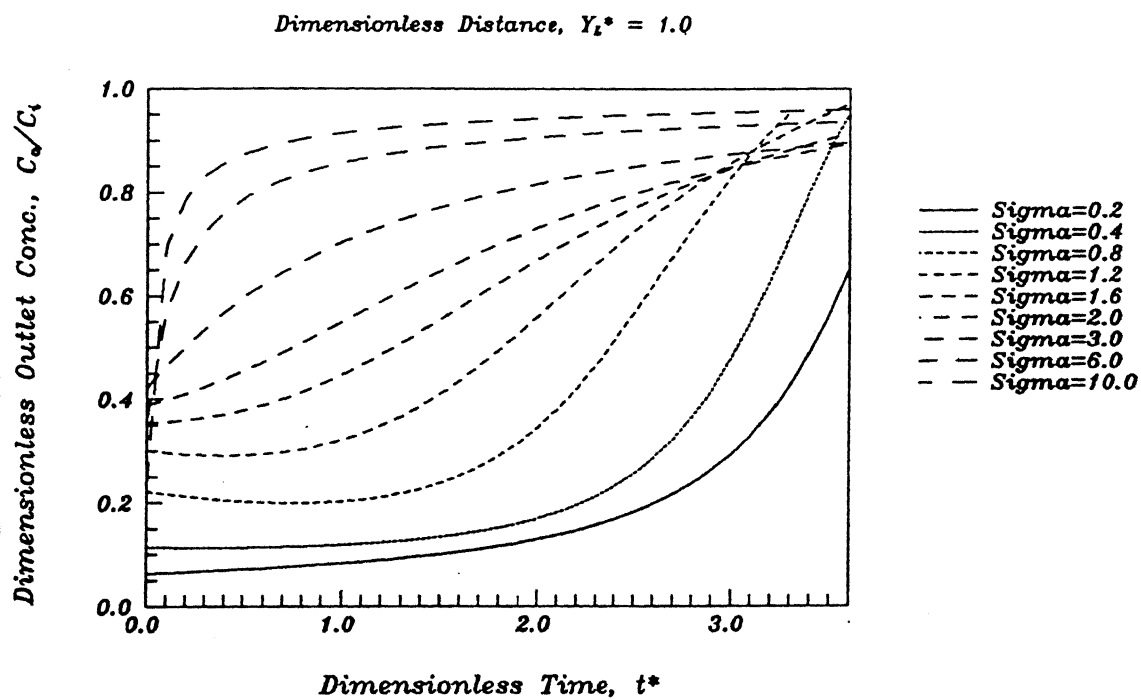


Figure 5.1: Predicted breakthrough curves for different values of dimensionless reaction modulus,  $\sigma$



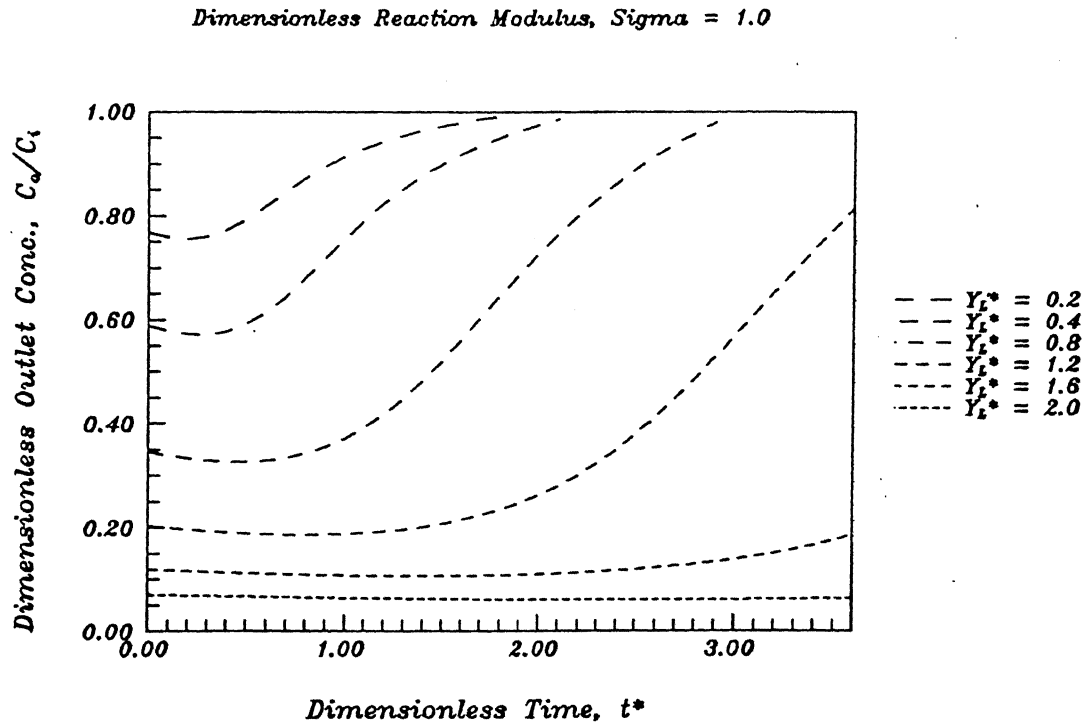


Figure 5.2: Predicted breakthrough curves for different values of dimensionless distance,  $y_L^*$

#### Effect of residence time

Greater the residence time, more would be the opportunity for the gas to remain in contact and react with the reactant solid and hence lesser would be the outlet concentration. Therefore, breakthrough curve would be delayed for large residence time and vice-versa.

From Equation 5.4, it is clear that greater the residence time, greater would be the value of  $y_L^*$ . From eqn. 5.1, outlet concentration would be smaller for greater  $y_L^*$  and ,hence, a delayed breakthrough curve.

#### Effect of $\omega$

More the amount of reactant solid in the packed bed, more would be the opportunity for the gas to react with it and result would be a delayed breakthrough curve.

Greater the value of  $\omega$ , greater would be the value of  $y_L^*$  and ,hence, a delayed breakthrough curve.

#### Effect of $\epsilon_v$

If the void fraction is more, gas solid contact would be less and it will lead to

higher outlet concentration or a quick breakthrough.

Greater the value of  $\epsilon_p$ , lesser would be the value of  $y_L^*$  and hence a quick breakthrough.

## 5.3 Comparison of predicted and experimental breakthrough curves for active sodium carbonate.

### 5.3.1 At different temperatures

Breakthrough curves are predicted at different temperatures 150, 200, 250, 300 and 350 °C. Inlet  $SO_2$  concentration and space velocity being 3500 ppm and 900  $hr^{-1}$ , respectively. Predicted breakthrough curves at different temperatures are shown in the Figure 5.3. These have been compared with the experimentally observed ones. Comparison is given in the Tables D.1-D.5 and shown in the Figures 5.4-5.8.

Rate constant and effective diffusivity are the two parameters which vary with temperature. Variation of these parameters with temperature are given in Appendix C. These values of rate constant and effective diffusivity were used for evaluating  $\sigma$  and  $y_L^*$  which in turn were used for predicting breakthrough curves. Effect of both the parameters is in the same direction.

As expected, predicted breakthrough curves are delayed and less sharp at higher temperature (Figure 5.3). It can also be seen from the Figures 5.4-5.8 that the predicted breakthrough curves match fairly well with the experimentally obtained ones except for  $T = 350$  °C. Departure of predicted breakthrough curves from the experimental one at 350 °C is attributed to the phenomenon of sintering. Sintering of pellets has been confirmed through scanning electron micrographs taken by Bhaskar (1994). Sintering results in a less porous and dense and compact solid reactant leading to poor diffusion into the reactant and, hence, poor reaction of gas with it.

### 5.3.2 At different Concentrations

Breakthrough curves are predicted at different inlet  $SO_2$  concentrations of 1500, 3500, 6000, 1800 ppm and at a temperature and space velocity of 200 °C and

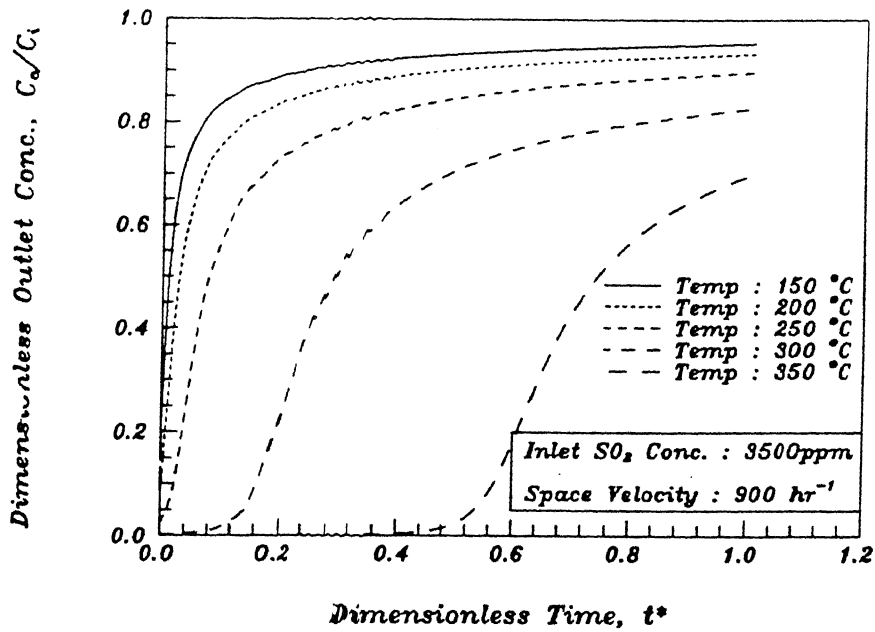


Figure 5.3: Predicted breakthrough curves for sulphation of active sodium carbonate at different temperatures, ( $C_A \approx 3500$  ppm)

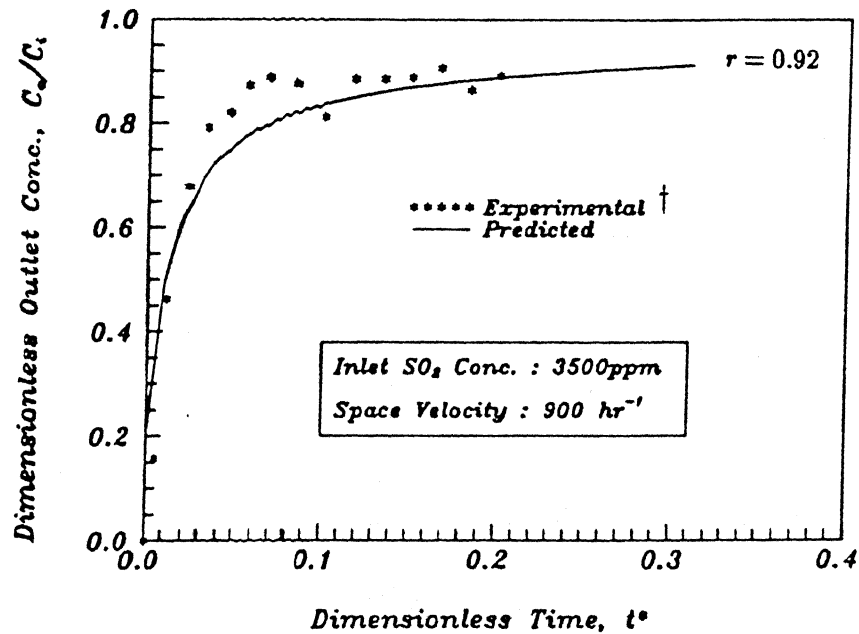


Figure 5.4: Breakthrough curve for sulphation of sodium carbonate at 150 °C.

† Source : Bhaskar,1994.

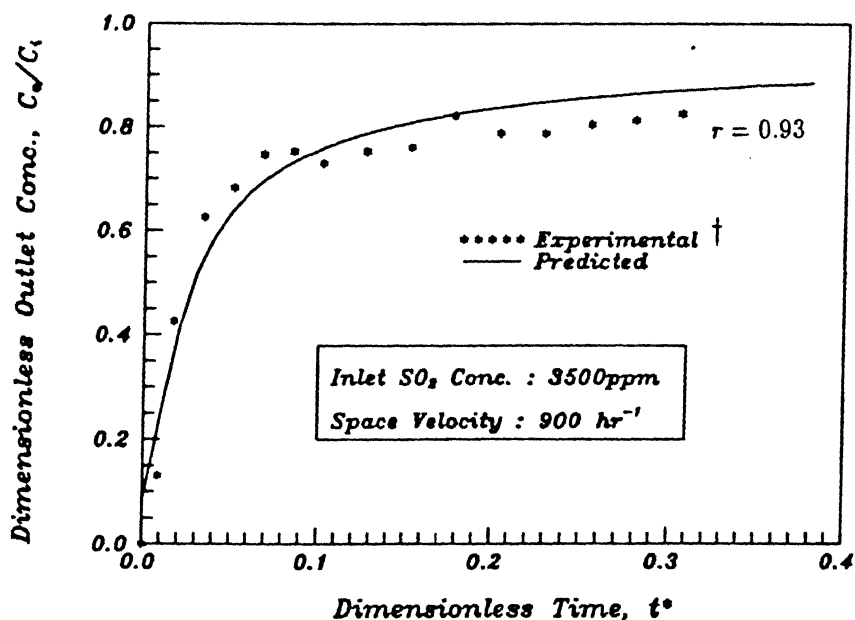


Figure 5.5: Breakthrough curve for sulphation of sodium carbonate at 200 °C.

† Source : Bhaskar,1994.

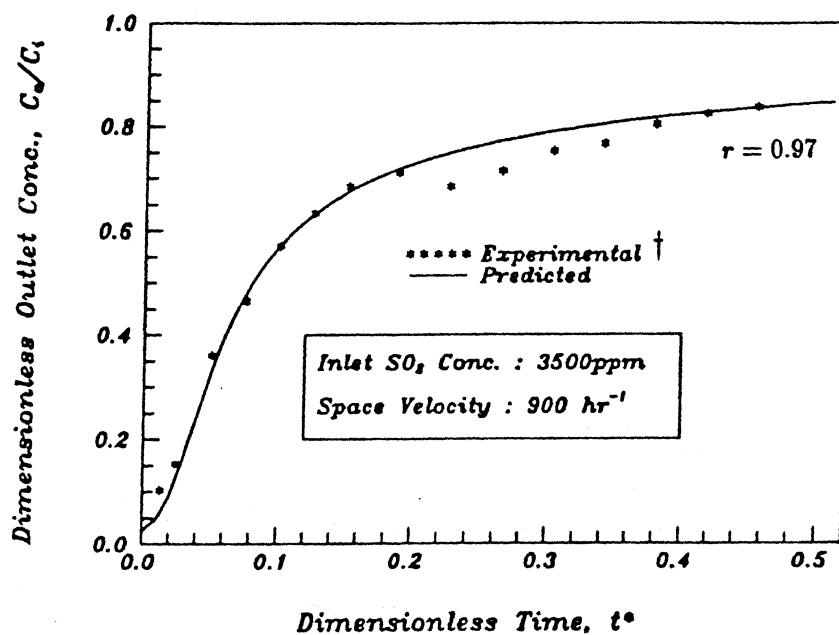
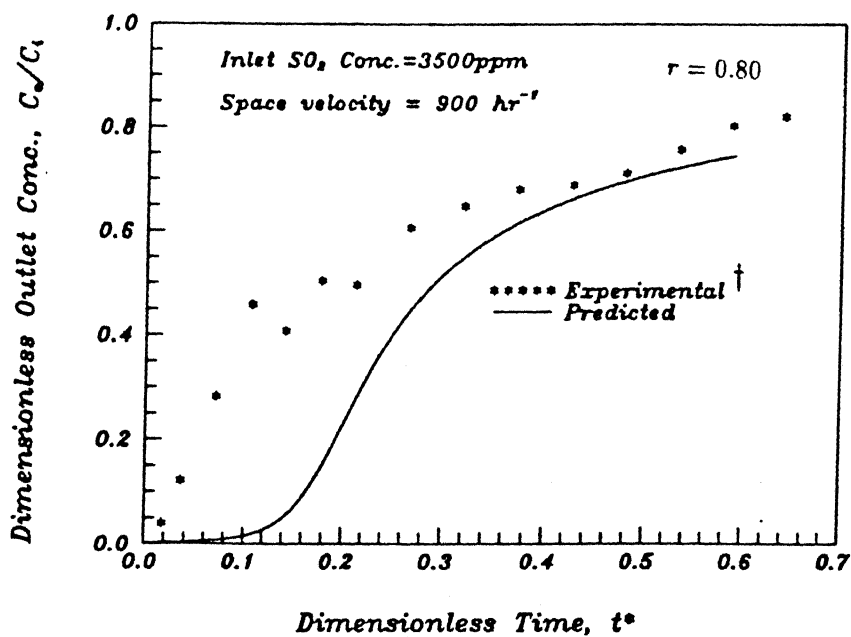
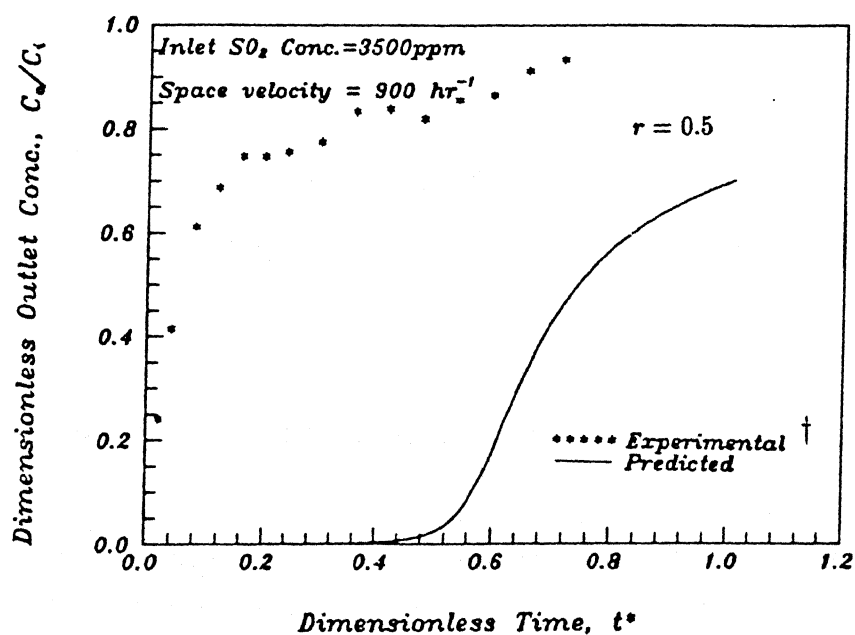


Figure 5.6: Breakthrough curve for sulphation of sodium carbonate at 250 °C.

† Source : Bhaskar,1994.

Figure 5.7: Breakthrough curve for sulphation of sodium carbonate at  $300^\circ\text{C}$ .

† Source : Bhaskar,1994.

Figure 5.8: Breakthrough curve for sulphation of sodium carbonate at  $350^\circ\text{C}$ .

† Source : Bhaskar,1994.

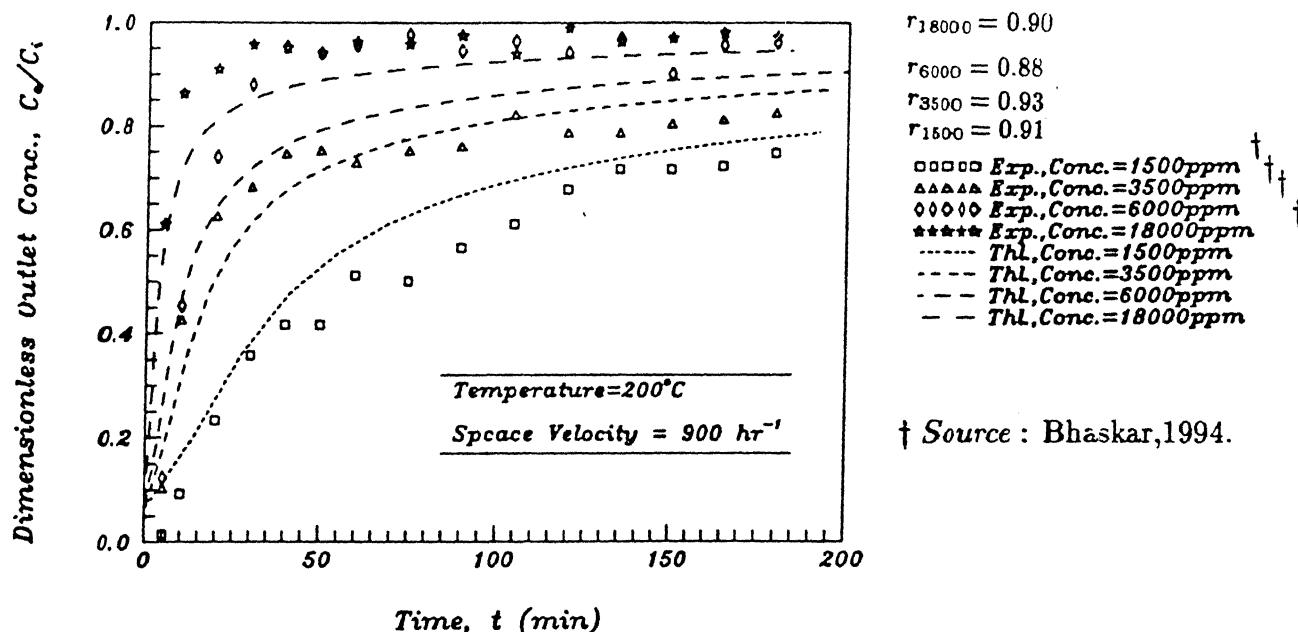


Figure 5.9: Breakthrough curves for sulphation of active sodium carbonate at different concentrations, ( $T = 200^\circ\text{C}$ )

$900 \text{ hr}^{-1}$ , respectively. Comparison of predicted and experimental breakthrough curves has been presented in Table D.6 and Figure 5.9. As expected, at higher values of inlet sulphur dioxide concentration, breakthrough has occurred faster. It is also seen that predicted curves match fairly well with the experimental ones.

## 5.4 Comparison of predicted and experimental breakthrough curves for calcined magnesium carbonate.

### 5.4.1 At different temperatures

Breakthrough curves have been predicted at different temperatures of 650, 750, and  $850^\circ\text{C}$ . Concentration and space velocity are 9000 ppm and  $600 \text{ hr}^{-1}$ , respectively. Predicted breakthrough curves at different temperatures are shown in Figure 5.10.

Predicted and experimental breakthrough curves have been compared and presented in Tables D.7-D.9 and Figures 5.11-5.13.

As expected, removal of sulphur dioxide is better at higher temperatures owing

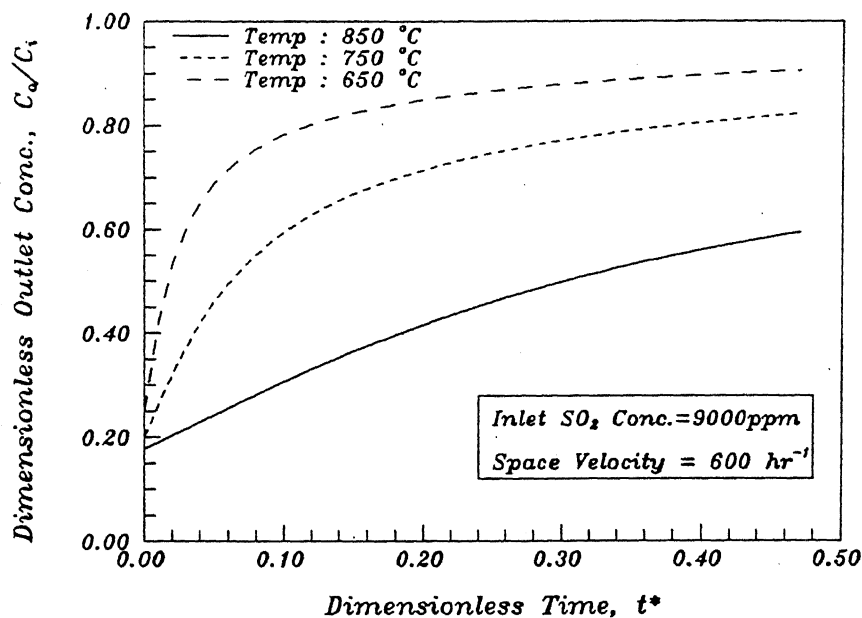


Figure 5.10: Breakthrough curves for sulphation of calcined magnesium carbonate at different temperatures, ( $C_{A_i} = 9000 \text{ ppm}$ )

to higher reaction rates and higher effective diffusivities. Experimental and predicted curves match fairly well except in the case of those at  $850^\circ\text{C}$ . Again, the reason for this departure is sintering which has not been accounted for in the model owing to less understanding of the phenomenon.

#### 5.4.2 At different Concentrations

Experimental and predicted breakthrough curves for sulphation of calcined magnesium carbonate at different concentrations of 2000, 9000, and 2200 ppm are presented in Table D.10 and Figure 5.14. Temperature and space velocity are  $750^\circ\text{C}$  and  $600 \text{ hr}^{-1}$ , respectively. Predicted curves match fairly well with the experimental ones and breakthrough is found to occur faster and sharper at higher inlet sulphur dioxide concentration.

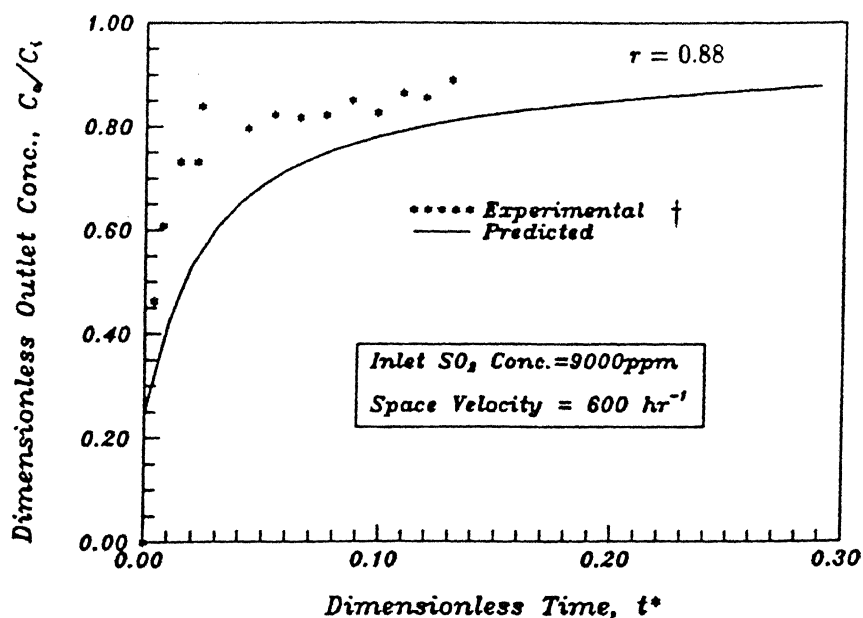


Figure 5.11: Breakthrough curves for sulphation of calcined magnesium carbonate at 650 °C.

† Source : Bhaskar,1994.

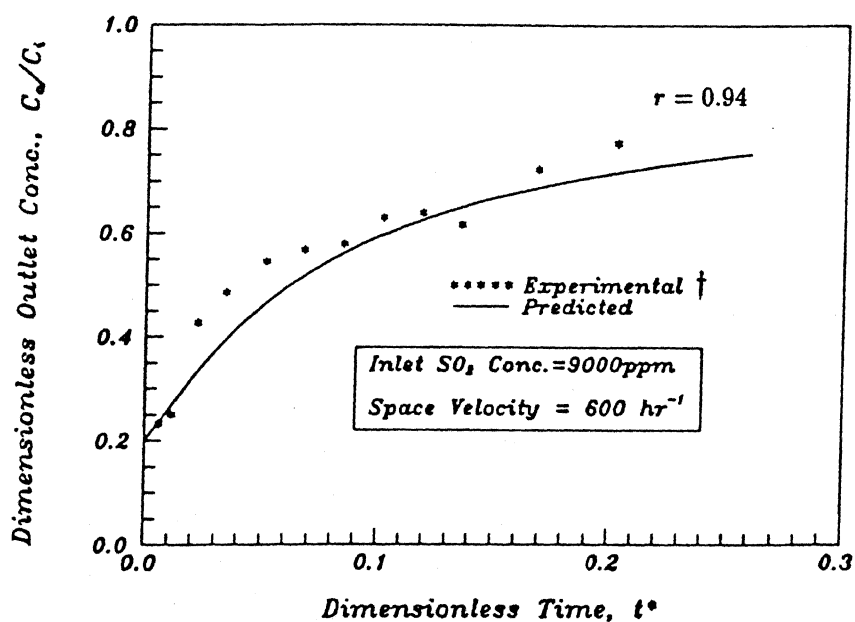


Figure 5.12: Breakthrough curves for sulphation of calcined magnesium carbonate at 750 °C.

† Source : Bhaskar,1994.



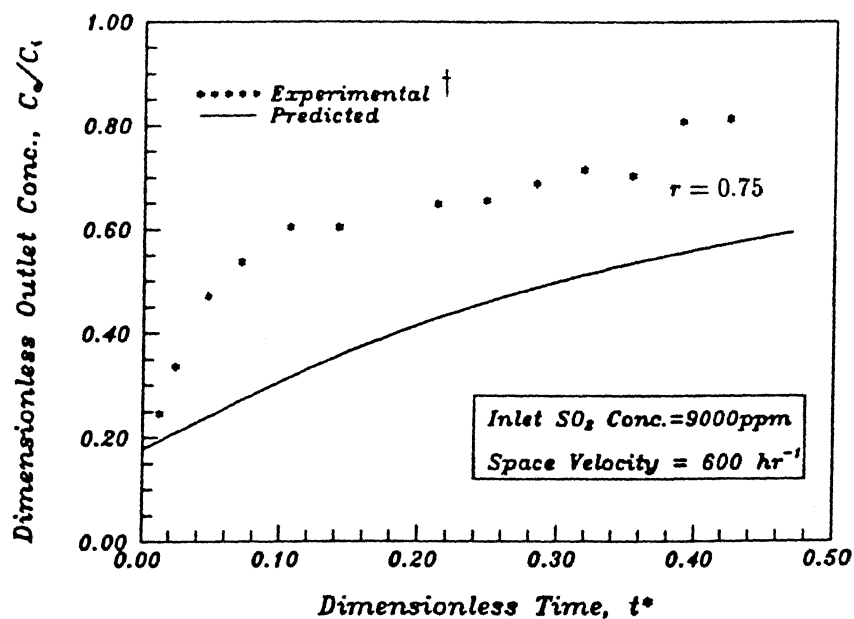


Figure 5.13: Breakthrough curves for sulphation of calcined magnesium carbonate at 850 °C.

† Source : Bhaskar, 1994.

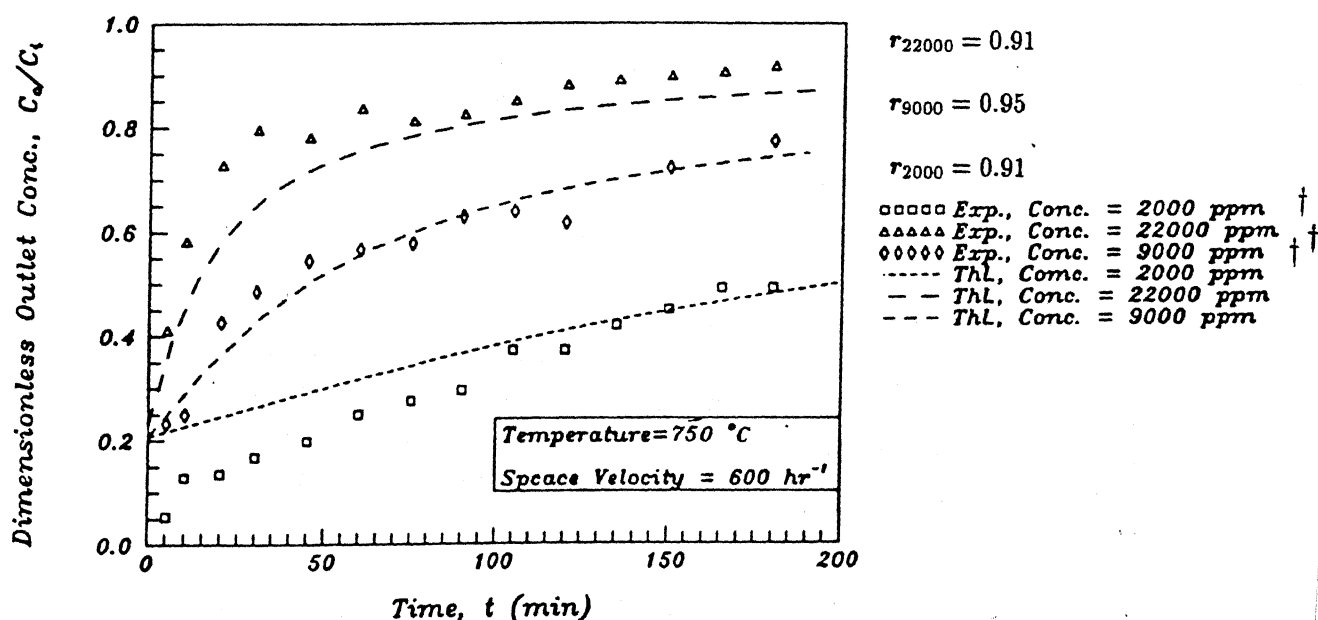


Figure 5.14: Breakthrough curves for sulphation of calcined magnesium carbonate at different concentrations, ( $T = 750$  °C)

† Source : Bhaskar, 1994.

## 5.5 Criticism of the present study

As is clear from the Equation 5.1, dimensionless outlet concentration varies exponentially with  $\beta$  and  $y_L^*$ . Theoretically, at time  $t=0$  dimensionless outlet concentration would be zero only if the product  $\beta y_L^*$  is infinity which is impractical. So, dimensionless outlet concentration would only be nearly equal to zero at time  $t=0$  as  $\beta$  or  $y_L^*$  or both become large which can be observed in the case of active sodium carbonate and sulphur dioxide system (especially at higher temperatures) and not so in the case of calcined magnesium carbonate and sulphur dioxide system.

From Equation 5.2 it is clear that  $\beta$  is inversely proportional to  $\sigma$ . As  $\sigma$  increases,  $\beta$  would decrease and vice-versa. Therefore, breakthrough would be delayed and less steep for small  $\sigma$  and vice-versa which is also supported by Figure 5.1. Then from Equation 5.3, one would be tempted to say that since  $\sigma$  is directly proportional to  $k$ , breakthrough would be delayed and less steep for smaller value of  $k$ . As is clear from the Equations 5.3 and 5.4, variation in  $k$  affects both  $\sigma$  as well as  $y_L^*$ . Effect of  $k$  on  $y_L^*$  is more than that on  $\sigma$  because  $y_L^*$  varies with  $k$  raised to the power 1 and  $\sigma$  varies with  $k$  raised to the power  $\frac{1}{2}$ . Therefore, effect of  $y_L^*$  due to variation of  $k$  on breakthrough curve would dominate that due to  $\sigma$  and, hence, breakthrough would be delayed and less steep for higher values of  $k$  and vice-versa. For other parameters (not explained in the sections 5.2 and 5.3) the breakthrough curves' trend can be explained on similar lines.

Figure 5.2 shows that breakthrough is quicker for smaller value of  $y_L^*$  or smaller value of  $k$  which is again supported by both the Equations 5.1 and 5.4.

Departure of simulated and experimental breakthrough curves may also be attributed to, besides sintering, change in porosity due to difference in molar volumes of the reactant and product (especially in the case of calcined magnesium carbonate and sulphur dioxide system), pore closure and changing effective diffusivity.

## Chapter 6

# Conclusions and Suggestions for Future Work

On the basis of the discussion presented in the last chapter it may be concluded that the model presented here for simulation of breakthrough curves in a packed bed reactor simulated fairly well the experimental results for the two solid reactants namely, active sodium carbonate and calcined magnesium carbonate. The observed departure of simulated results from the experimental data, especially, at higher temperatures in the case of both the sorbents may be attributed to the structural changes such as sintering, change in porosity etc. occurring in the solid reactant during the course of the reaction.

A more comprehensive model which takes into account the non-isothermal conditions and structural changes should be developed for better simulation.

With the help of computer, a number of sets of curves may be obtained by varying different parameters involved one by one. Then to get predicted breakthrough curves for a specific reactant and under different process conditions, interpolation may be resorted to.

# References

Alvfors, P. and Svedberg, G. (1988). Modelling of the Sulphation of Calcined Limestone and Dolomite - A Gas-Solid Reaction with Structural Changes in the Presence of Inert Solids, *Chemical Engineering Science*, Vol. 43, pp. 1183-1193.

Aris, R. and Amudson, N.R. (1973). Mathematical Methods in Chemical Engineering Vol. 2; *First Order Differential Equations with Applications*, Prentice Hall, Englewood Cliffs, New Jersey, USA.

Bhaskar, P.U. and Ghosh, D.K. (1994). Kinetics of Sulphur Dioxide Removal with Active Sodium Carbonate, *Proceedings of International Symposium on 'Instrumentation and Control of Environmental Pollution'*, Indian Instrumentation Scientists and Technologists, Jadavpur University, calcutta, India, pp. 25-32.

Bhaskar, P.U. (1994). Evaluation of Active Sodium Carbonate and Calcined Magnesium Carbonate for Dry Flue Gas Desulphurisation , *Ph.D. thesis*, Indian Institute of Technology, Kanpur, India.

Borgwardt, R.H. and Harvey, R.D. (1972). Properties of Carbonate Rocks Related to Sulphur Dioxide Reactivity, *Environmental Science and Technology*, Vol. 6, pp. 350-360.

Borgwardt, R.H. (1970). Kinetics of the Reaction of Sulphur dioxide with Calcined Limestone, *Environmental Science and Technology*, Vol. 4, pp.59-63.

Dam Johansen, K., Hansen, P.F.B. and Ostergaard, K. (1991). High Temperature Reaction between Sulphur Dioxide and Limestone III; A Grain-Micrograin Model and its verification, *Chemical Engineering Science*, Vol 46, No.3, pp. 847-853.

Ghosh, D.K., and Maiti, B.R. (1989). Kinetics of Sulphation with Calcined Dolomite and Packed Bed Modelling for the system, in *Recent Advances in Chemical Engineering*, D.N. Saraf and D. Kunzru (editors), Tata McGraw-Hill Publishing Company Limited, New Delhi, India.

Hartman, M. and Coughlin, R.W. (1974). Reactin of Sulphur Dioxide with Limestone and the Influence of Pore Structure, *Industrial Engineering Chemistry Process Design and Develpment*, Vol. 13, pp.248-253.

Hartman, M. and Coughlin, R.W. (1976). Reaction of Sulphur Dioxide with Limestone and the grain Model, *AIChE Journal*, Vol. 22, pp. 490-498.

Karlegard, A. and Bjerle, I. (1994). Kinetic Studies on High Temperature Desulphurisation of Synthesis Gas with Zinc Ferrite, *Chem. Eng. Technol.*, Vol 17, pp21-29.

Levenspiel, O. (1972). *Chemical Reaction Engineering*, Second Edition, Wiley Eastern Limited.

Marrier, P. and Dibles, H.P. (1974). The Catalytic Conversion of  $SO_2$  to  $SO_3$  by Fly Ash and Capture of  $SO_2$  and  $SO_3$  by CaO and MgO, *Thermochemica Acta*, Vol. 8, pp. 155-165.

Offen, G.R., McElroy, M.W. and Muzio, L.J. (1987). Assessment of Dry Sorbent Emission Control Technologies, part 2-Applications, *Journal of Air Pollution Control Association*, Vol. 37, pp. 968-980.

Pigford, R.L. and Sliger, G. (1973). Rate of Diffusion Controlled Reaction between a Gas and a Porous Solid Sphere - Reaction of  $SO_2$  with  $CaCO_3$ , *Industrial Engineering Chemistry Process Design and Development*, Vol. 12, No. 1, pp. 85-91.

Ranade, M.G. and Evans, J.W. (1980). The Reaction between a Gas and a Solid in a Non-isothermal Packed Bed: Simulations and Experiments, *Industrial Engineering Chemistry Process Design and Development*, Vol. 19, pp. 118-123.

Stern, A.C. (Ed.) (1977). *Air Pollution Vol. 4 - Engineering Control of Air Pollution*, Third Edition, Academic Press Inc., New York, USA.

Stern, A.C., Boubel, R.W.; Turner, D.B. and Fox, D.L. (1984). *Fundamentals of Air Pollution*, Second Edition, Academic Press Inc., New York, USA.

Szekely, J., Evans, J.W. and Sohn, H.Y. (1976). *Gas Solid Reactions*, Academic Press, New York, USA.

Wark, K. and Warner C.F. (1981). *Air Pollution - Its Origin and Control*, Harper and Row publishers, New York, USA.

# Appendix A

## Source Code of the Software Package

```
#include <starbase.c.h>
#include <math.h>
#include <stdio.h>
#include <stdlib.h>
#include <string.h>
#define Edge TRUE
#define SimplexSansSerif 4
#define BoldSansSerif 6
#define EndOfLine FALSE

struct s1 { char *fnt1,
    *fnt2,
    *fnd;
    } filename[10] = {
{"t1.1", "t1.2", "d1.o"},
{"t2.1", "t2.2", "d2.o"},
{"t3.1", "t3.2", "d3.o"},
{"t4.1", "t4.2", "d4.o"},
{"t5.1", "t5.2", "d5.o"},
{"t6.1", "t6.2", "d6.o"},
{"t7.1", "t7.2", "d7.o"},
{"t8.1", "t8.2", "d8.o"},
{"t9.1", "t9.2", "d9.o"},
{"t10.1", "t10.2", "d10.o"}
};
FILE *ptdatain,*ptdatain1,*ptdataout[20],*pttextout1[20],
    *pttextout2[20], *original, *datafile[10];
char xstring1[50]="DIMENSIONLESS TIME t*",
    xstring2[50]="TIME (min.)",
    ystring1[50]="DIMENSIONLESS OUTLET CONC. Co/Ci",
```

[illegible]

```

printf("\nENTER THE MAIN TITLE : ");
printf("\nENTER\n\t\'1\'\tFOR  \"BREAKTHROUGH  CURVES\"\n\t\'
2\'\tFOR ENTERING SOME OTHER\n ? ");
scanf("%c",&r);
scanf("%c",&dummy);
if(r=='1')
    strcpy(main_title,mainstring1);
if(r=='2')
    gets(main_title);
printf("\nENTER THE X-AXIS TITLE : ");
printf("\nENTER\n\t\'1\'\tFOR  \"DIMENSIONLESS  TIME t* \"\n
\t\'2\'\tFOR  \"TIME (min) ->\"\n\t\'3\'\tFOR ENTERING
SOME OTHER\n ? ");
scanf("%c",&r);
scanf("%c",&dummy);
if(r=='1')
    strcpy(x_title,xstring1);
else if(r=='2')
    strcpy(x_title,xstring2);
else
    gets(x_title);
printf("\nENTER THE Y-AXIS TITLE : ");
printf("\nENTER\n\t\'1\'\tFOR  \"DIMENSIONLESS OUTLET CONC.
Co/Ci \"\n\t\'2\'\tFOR  \"FRACTIONAL CONVERSION X\"\n\t\'
3\'\tFOR ENTERING SOME OTHER\n ? ");
scanf("%c",&r);
scanf("%c",&dummy);
if(r=='1')
    strcpy(y_title,ystring1);
else if(r=='2')
    strcpy(y_title,ystring2);
else
    gets(y_title);
for(j=0;j<tn;j++)
{
    printf("\nENTER THE TITLE FOR THE %dst CURVE\n(DEFAULT IS THE
FILENAME) : ",j+1);
    gets(legend[j]);
    if(strlen(legend[j]) <= 2)
        /* legend[j] = fname[j]; */
        strcpy(legend[j],fname[j]);
}
printf("\nDO YOU WANT TO ENTER THE VALUE OF THE DIVIDER?\n\
\DEFAULT VALUE OF DIVIDER IS 100. RUN THE PROGRAM\n\
\ONCE WITH DEFAULT VALUE. IF THE SIZE OF TICS IS\n\
\RLARGE,NEXT TIME, ENTER A VALUE > 100 FOR THE DIVIDER\n\
\RAND VICE VERSA.\n\n(y/n) : ");
scanf("%c",&r_divider);
scanf("%c",&dummy);
if (r_divider == 'y')
    { printf("\nENTER THE VALUE OF DIVEREDER : ");

```



```

        scanf("%d",&divider);
        scanf("%c",&dummy);
    }

/***** setting parameters *****/

for (m=0;m<tn;m++)
{
    i=1;
    k=1;
    datafile[m] =fopen(fname[m],"r");
    fscanf(datafile[m],"%f%f",&X,&Y);
    x_data[m][0]=X;
    y_data[m][0]=Y;
    while(fscanf(datafile[m], "%f%f", &X, &Y) != EOF)
    {
        x_data[m][i++]=X;
        y_data[m][k++]=Y;
    }
    N[m]=i;
    xmax=x_data[m][0];
    ymax=y_data[m][0];
    xmin=x_data[m][0];
    ymin=y_data[m][0];
    for(i=1,j=1; i<N[m] ; i++,j++)
    {
        if (x_data[m][i] > xmax) xmax=x_data[m][i];
        if (y_data[m][j] > ymax) ymax=y_data[m][j];
    }
    local_x_max[m]=xmax;
    local_y_max[m]=ymax;
    for(i=1,j=1; i<N[m] ; i++,j++)
    {
        if (x_data[m][i] < xmin) xmin=x_data[m][i];
        if (y_data[m][j] < ymin) ymin=y_data[m][j];
    }
    local_y_min[m]=ymin;
    local_x_min[m]=xmin;
    fclose(datafile[m]);
}

/*****/

for(i=0;i<tn;i++)
printf("\nNUMBER OF DATA IN THE FILE %s = %d",fname[i],N[i]);
xmax=local_x_max[0];
ymax=local_y_max[0];
xmin=local_x_min[0];
ymin=local_y_min[0];
for(i=1,j=1;i<tn;i++,j++)
{

```

```

        if (local_x_max[i] > xmax) xmax=local_x_max[i];
        if (local_y_max[j] > ymax) ymax=local_y_max[j];
    }
    abs_x_max = xmax;
    abs_y_max = ymax;
    for (i=1,j=1;i<tn;i++,j++)
    {
        if(local_x_min[i] < xmin)  xmin=local_x_min[i];
        if(local_y_min[j] < ymin)  ymin=local_y_min[j];
    }
    abs_x_min = xmin;
    abs_y_min = ymin;

/*****/

delta_x = (abs_x_max - abs_x_min)/divider;
delta_y = (abs_y_max - abs_y_min)/divider;
x_ticsize = delta_y;
y_ticsize = delta_x;
printf("\n\nPRESENT CO-ORDINATE LIMITS ARE : \n\n");
printf("\n\nABS-X-MIN = %f\nABS-Y-MIN = %f\nABS-X-MAX = %f\nABS-Y-
    -MAX = %f\n\n",abs_x_min,abs_y_min,abs_x_max,abs_y_max);
printf("\nDO YOU WANT TO CHANGE THESE LIMITS ? (y/n) : ");
scanf("%c",&r);
scanf("%c",&dummy);
if(r=='y')
{
    printf("\n\nX-MIN = ");
    scanf("%f",&abs_x_min);
    scanf("%c",&dummy);
    printf("\n\nY-MIN = ");
    scanf("%f",&abs_y_min);
    scanf("%c",&dummy);
    printf("\n\nX-MAX = ");
    scanf("%f",&abs_x_max);
    scanf("%c",&dummy);
    printf("\n\nY-MAX = ");
    scanf("%f",&abs_y_max);
    scanf("%c",&dummy);
}
if((abs_x_max==abs_x_min) || (abs_y_max==abs_y_min))
{ printf("\n\nmax value = min value\n\n");
  exit(-1);
}
/*for(j=0; j<=n; j++)
printf("x[%d] = %f   y[%d] = %f \n",j,x_data[j],j,y_data[j]); */

/*****/

printf("\nEnter the device type\ ' ?\n\nENTER\n\t\ 'ws\ '\tFOR
    WORKSTATION\n\t\ 'srx\ '\tFOR \ 'SRX\ '\n\t\ 'tsrx\ '\tFOR

```

```

        \ 'TSRX\ ' \n \n \t? ");
gets(r_device);
if(strcmp(r_device,"ws")==0)
    r_d='1';
else if(strcmp(r_device,"srx")==0)
    r_d='2';
    else if(strcmp(r_device,"tsrx")==0)
        r_d='3';
    else printf("\n\nERROR IN INITIALISING DEVICE TYPE\n\n");
switch(r_d)
{
    case '1' :
        term_type = ws;
        printf("TERM = %s\n",ws);
        break;
    case '2' :
        term_type = srx;
        printf("TERM = %s\n",srx);
        break;
    case '3' :
        term_type = tsrx;
        printf("TERM = %s\n",tsrx);
        break;
}

/***** Input of main,x-axis,y-axis titles *****/

printf("\nWANT TO VIEW THE GRAPH\nOR\nWANT TO CREATE THE PLOT
FILE\ TO BE PLOTTED ON THE PLOTTER \n\nENTER\n\n\t\'1\'
\tFOR\ VIEWING THE GRAPH FIRST AND THEN\n\t\tCREATING THE
PLOT FILE\ \n\n\t\'2\' \tFOR CREATING THE PLOT FILE ONLY.
\n\n\t? ");
r1=getchar();
scanf("%c",&dummy);
printf("\nWAIT !\n");
if(r1=='1' && ag=='n')
{
    printf("\n\ 'DO YOU WANT TO HAVE THE BITMAP FILE FOR PRINTING\'
(y/n) : ");
    scanf("%c",&r_bit);
    scanf("%c",&dummy);
    if(r_bit=='y')
    {
        printf("\n\n\ 'ENTER THE NAME OF THE BITMAP-FILE\' : ");
        scanf("%s",bit_filename);
        scanf("%c",&dummy);
        lenb=strlen(bit_filename);
        for(i=0;i<5;i++)
            bit_filename[lenb+i] = bit[i];
        printf("\nWAIT !\n");
    }
}

```

```

    else
    printf("\nWAIT !\n");
}
again : if(ag=='y')
    {
        r1='2';
    }
if(r1=='2')
{
    printf("\n\nENTER THE NAME OF THE PLOT FILE : ");
    scanf("%s",plot_filename);
    lenp=strlen(plot_filename);
    scanf("%c",&dummy);
    for(i=0;i<5;i++)
        plot_filename[lenp+i] = plt[i];
    printf("\nWAIT !\n");
}
switch(r1)
{
case '1' :
    printf("\33h\33j"), fflush(stdout);
    if((fildes=gopen("/dev/crt",OUTDEV,term_type,INIT))==
        exit(-1);
    system("clear");
    break;
case '2' :
    system("clear");
    printf("\tWAIT !\n");
    if((fildes=gopen(plot_filename,OUTDEV,"hpgl",SPOOLED))===-1)
        exit(-1);
    break;
}
buffer_mode(fildes,TRUE);

/***** SELECTING VIEWPORT, WINDOW ETC. *****/

vdc_extent(fildes,0.0,0.0,0.0,1.25,1.0,0.0);
view_port(fildes,0.35*1.25,0.35,0.95*1.25,0.85);
view_window(fildes,abs_x_min,abs_y_min,abs_x_max,abs_y_max);
interior_style(fildes,INT_HOLLOW,Edge);
rectangle(fildes,abs_x_min,abs_y_min,abs_x_max,abs_y_max);

/***** PLOTTING GRAPH *****/

k=0;
i=0;
for (j=0;j<tn;j++)
{
    printf("\n\nCOLOUR INDEX CAN HAVE VALUE RANGING FROM 0-256.\n\n\
        COLOURS AVAILABLE ON THE PLOTTER ARE FROM 0-7.\n\n\
        COLOUR          INDEX\n\n\

```

```

                                \n\
WHITE                          1\n\
RED                            2\n\
YELLOW                        3\n\
GREEN                        4\n\
CYAN                         5\n\
BLUE                         6\n\
MAGENTA                      7");
printf("\n\nCOLOUR INDEX FOR THE FILE %s : ",fname[j]);
scanf("%d",&colour_index); /*
datafile[j] =fopen(fname[j],"r");
fscanf(datafile[j],"%f%f",&X,&Y);
move2d(filides,X,Y);
while(fscanf(datafile[j], "%f%f", &X, &Y) != EOF)
{
    if(j==6.) k=0;
    if(j==6.) i=0;
    line_type(filides,i);
    line_color_index(filides,2+k);
    draw2d(filides,X,Y);
}
i++;
k++;
fclose(datafile[j]);
}

/***** do the main title *****/

interior_style(filides,INT_SOLID,Edge);
text_font_index(filides,SimplexSansSerif);
text_alignment(filides,TA_CENTER,TA_CENTER,0.,0.);
character_height(filides,.03);
text_color_index(filides,4);
text2d(filides,0.65*1.25,.93,main_title,VDC_TEXT,EndOfLine);

/***** do the x-axis title *****/

text_font_index(filides, SimplexSansSerif);
text_alignment(filides,TA_CENTER,TA_CENTER,0.,0.);
character_height(filides,.03);
text_color_index(filides,4);
text2d(filides,0.65*1.25,0.3,x_title,VDC_TEXT,EndOfLine);

/***** do the y-axis title *****/

text_font_index(filides, SimplexSansSerif);
text_alignment(filides,TA_CAP,TA_CENTER,0.,0.);
character_height(filides,.03);
text_orientation2d(filides, -1.0 ,0. ,0. ,1.0);
text_color_index(filides,4);
text2d(filides,0.27*1.2,0.6,y_title,VDC_TEXT,EndOfLine);

```

```

/***** TIC MARKS *****/
line_color_index(fildes,4);
clip_indicator(fildes,CLIP_TO_VIEWPORT);
Tics(fildes,'X',abs_y_min,abs_x_min,abs_x_max,delta_x,x_ticsize,10);
Tics(fildes,'X',abs_y_max,abs_x_min,abs_x_max,delta_x,x_ticsize,10);
Tics(fildes,'Y',abs_x_min,abs_y_min,abs_y_max,delta_y,y_ticsize,10);
Tics(fildes,'Y',abs_x_max,abs_y_min,abs_y_max,delta_y,y_ticsize,10);

/***** label the X tic labels *****/
clip_indicator(fildes,CLIP_TO_VDC);
text_orientation2d(fildes,0.0,1.0,1.0,0.0);
character_height(fildes, 4 * delta_y );
character_width(fildes,1.5 * delta_x);
text_color_index(fildes,4);
text_alignment(fildes,TA_CENTER,TA_TOP,0.0,0.0);
for(X=abs_x_min;X<=abs_x_max;X+=10.0 * delta_x)
{
    if(abs_x_max<=10.)
        sprintf(Strng, "%5.2f",X);
    else if(abs_x_max<=40.)
        sprintf(Strng, "%4.1f",X);
    else
        sprintf(Strng, "%4.0f",X);
    text2d(fildes,X,abs_y_min,Strng,WORLD_COORDINATE_TEXT,EndOf
        Line);
}
sprintf(Strng, "%5.1f", abs_x_max);
text2d(fildes,abs_x_max,abs_y_min,Strng,WORLD_COORDINATE_TEXT
    ,EndOfLine);

/*****label the Y tic labels *****/
text_alignment(fildes,TA_RIGHT,TA_HALF,0.0,0.0);
text_color_index(fildes,4);
for(Y=abs_y_min;Y<=abs_y_max + delta_y;Y+=10.0 * delta_y)
{
    if(abs_y_max<=10.)
        sprintf(Strng, "%5.2f ",Y);
    else if(abs_y_max<=40.)
        sprintf(Strng, "%4.1f",Y);
    else
        sprintf(Strng, "%4.0f",Y);
    text2d(fildes,(abs_x_min-2.*delta_x),Y,Strng,WORLD_COORDINATE
        _TEXT,EndOfLine);
}
flush_buffer(fildes);

/***** viewing graph *****/

```

```

/* printf("PRESS ENTER TO VIEW THE GRAPH\n");
scanf("%c",&dummy);
printf("\nDO YOU WANT TO CLEAR THE SCREEN BEFORE VIEWING GRAPH
(y/n) : ");
scanf("%c",&r);
if(r=='y')
system("clear"); */

```

```

/***** SECOND VIEW PORT FOR LEGEND *****/

```

```

vdc_extent(fildes,.0,.0,.0,1.25,1.,.0);
view_port(fildes,0.4*1.25,0.05,0.98*1.25,0.25);
view_window(fildes,.0,.0,100.,100.);
interior_style(fildes,INT_HOLLOW,Edge);
text_font_index(fildes,SimplexSansSerif);
text_alignment(fildes,TA_LEFT,TA_CENTER,0.,0.);
character_height(fildes,10.);
character_width(fildes,1.8);
k=0;
i=0;
for(j=0;j<tn;j++)
{
    if(j>13)
        break;
    if(j==6)
    {
        k=0;
        i=0;
    }
    if(j>=6)
    {
        line_type(fildes,i);
        line_color_index(fildes,k+2);
        move2d(fildes,60.0,90.-(5.+12.*i));
        draw2d(fildes,70.0,90.-(5.+12.*i));
        text_color_index(fildes,2);
        text2d(fildes,75.0,90.-(5.+12.*i),legend[j],WORLD_COORDINATE
        _TEXT,EndOfLine);
        k++;
        i++;
        continue;
    }
    line_type(fildes,i);
    line_color_index(fildes,k+2);
    move2d(fildes,5.0,90.-(5.+12.*i));
    draw2d(fildes,20.0,90.-(5.+12.*i));
    text_color_index(fildes,2);
    text2d(fildes,25.0,90.-(5.+12.*i),legend[j],WORLD_COORDINATE
    _TEXT,EndOfLine);
    k++;
}

```

```

        i++;
    }
    make_picture_current(fildes);
    flush_buffer(fildes);

/***** Third view port *****/

    vdc_extent(fildes,.0,.0,.0,1.25,1.,.0);
    view_port(fildes,0.4*1.25,0.0,0.98*1.25,0.05);
    view_window(fildes,.0,.0,60.,5.);
    interior_style(fildes,INT_HOLLOW,Edge);
    text_font_index(fildes,SimplexSansSerif);
    text_alignment(fildes,TA_CENTER,TA_CENTER,0.,0.);
    character_height(fildes,2.75);
    character_width(fildes,1.2);
    text_color_index(fildes,2);
    text2d(fildes,30.0,2.5,"DEVELOPED BY SATISH KUMAR",WORLD_COORDIN
ATE_TEXT,EndOfLine);
    make_picture_current(fildes);

/***** CREATING BITMAP FILE *****/
    if(r1=='1' && ag=='n' && r_bit=='y')
    {
        printf("\nWAIT !\n");
        bitmap_to_file(fildes,
TRUE,
0,
0,
bit_filename,
TRUE,
.25,1.,820,1000,
TRUE);
    }

/***** CLEARING SCREEN FOR THE IMAGE *****/

    /* system("clear");*/
    /* make_picture_current(fildes); */
    /*sleep(2); */

/***** RETRIEVING IMAGE FROM THE FILE *****/

    /* file_to_bitmap(fildes,*/
/* TRUE,      */
/* 0,0,      */
/* bit_filename, */
/* 0.0,1.0,  */
/* TRUE); */

/***** CLOSING THE DEVICE *****/

```



```

if(r1=='1')
{
if (fclose(fildes)==0)
    printf("file closed successfully.\n");
else
    printf("Error in closing file.\n");
printf("\nDO YOU WANT TO CREATE PLOT FILE ? (y/n) : ");
ag=getchar();
scanf("%c",&dummy);
if(ag=='y')
    goto again;
}
if(ag=='y')
if (fclose(fildes)==0)
    printf("file closed successfully.\n");
else
    printf("Error in closing file.\n");

printf("\n\n\n'END OF THE PROGRAMME'\n\n\n");
}
/***** SUBROUTINE Tics *****/

Tics(fildes,Axis,Location,Start,End,Delta,Size,Major)
int fildes;
char Axis;
float Location,
      Start,
      End,
      Delta,
      Size;
int Major;

#define Len (Tic%Major!=0 ? Size : 2.0*Size)
#define move 0.0
#define draw 1.0
{
    int Tic;
    float X,Y;
    float TicMks[1200];
    float *TicPtr;
    TicPtr=TicMks;
    switch (Axis){
        case 'X' : case 'x':
            for(X=Start,Tic=0;X<=End;X+=Delta,Tic++)
            {
                *TicPtr++ =X,*TicPtr++=Location-Len,*TicPtr++=move;
                *TicPtr++ =X,*TicPtr++=Location+Len,*TicPtr++=draw;
            }
            break;
        case 'Y' : case 'y':
            for(Y=Start,Tic=0;Y<=End;Y+=Delta,Tic++)

```

```

{
    *TicPtr++ =Location-Len,*TicPtr++=Y,*TicPtr++=move;
    *TicPtr++ =Location+Len,*TicPtr++=Y,*TicPtr++=draw;
}
break;
}
polyline2d(fildes,TicMks,(TicPtr-TicMks) / 3,TRUE);
}

/*****/

void prt()
{
    char dummy;
    printf("
\r*****
\r*****
\r*****
\r*****          NAME OF THE STUDENT :   SATISH KUMAR          *****
\r*****          *****
\r*****          THESIS SUPERVISOR   :   Dr. D.K. GHOSH          *****
\r*****          *****
\r*****
\r*****          *****\n\
*****\n\
***          ***\n\
***          TITLE          ***\n\
***          ***\n\
\r*****
\r*****
\r**          **
\r**          SIMULATION OF BREAKTHROUGH   CURVES FOR DRY          **
\r**          **
\r**          DESULPHURIZATION OF FLUE GAS USING          *
\r**          *
\r**          CALCINED MAGNESIUM CARBONATE          **
\r**          **
\r*****
\r*****
printf("\nPress ENTER ... \n");
scanf("%c",&dummy);
system("clear");
printf("
}

/*****/

void diff1()
{
    float be1();

```

```

float fn1();
void solve1();
printf("\nENTER\n\t\t'1'\t\tIF YOU WANT TO ENTER DATA FROM THE
TERMINAL\n\t\t'2'\t\tIF THROUGH DATAFILE\n ? ");
scanf("%c",&r1);
scanf("%c",&dummy);
printf("\nWAIT !\nWRITING FILE \"data1.in\"\n");
if(r1=='2')
{
printf("\nENTER THE NAME OF DATA-INPUT FILE : ");
scanf("%s",datain);
scanf("%c",&dummy);
ptdatain1 = fopen(datain,"a+");
/* system("cp data1.in d.in"); */
}
/*original = fopen("original","w"); */
/* if(r1=='2')
{
fprintf(ptdatain1,"\n\nENTER THE VALUES OF THE PARAMETERS IN
THE STRICT ORDER GIVEN\n");
fprintf(ptdatain1,"BELOW. DATA CAN BE ENTERED IN A LINE ONE
AFTER THE OTHER\n");
fprintf(ptdatain1,"SEPARATED BY SPACE.\n");
fprintf(ptdatain1,"DATA SHOULD BE ENTERED ONLY ABOVE THIS TEXT.
\n");
fprintf(ptdatain1,"MORE THAN ONE DATA SETS CAN BE ENTERED. BEGI
NING OF A NEW\n");
fprintf(ptdatain1,"SET SHOULD BE STARTED FROM A NEW LINE FOR
CLARITY.\n\n");
fprintf(ptdatain1,"OUTPUT FILES WILL BE GENERATED CORRESPONDING
TO EACH\n");
fprintf(ptdatain1,"SET OF DATA.\n\n");
fprintf(ptdatain1,"1. VALUE OF SIGMA\n");
fprintf(ptdatain1,"2. VALUE OF YLst(dimensionless distance)\n");
fprintf(ptdatain1,"3. h, STEP INCREMENT IN THE INDEPENDENT
VARIABLE TIME\n");
fprintf(ptdatain1,"4. TMAX, MAXIMUM VALUE OF INDEPENDENT VARIAN
LE UPTO WHICH\nDIFF. EQ. IS TO BE INTEGRATED\n");
fclose(ptdatain1);
} */
printf("\n\nTWO TYPE OF OUTPUT FILES WILL BE GENERATED BY THIS
PROGRAM\n\n\
1. HAVING NAME AS d(n).o WHERE 'n' DENOTES THE NO. OF THE FILE
.\n\
THIS FILE CONTAINS VARIATION OF DIMENSIONLESS OUTLET CONC.
WITH\n\
DIMENSIONLESS TIME.\n\
2. t(n).1 THIS FILES GIVES VALUES OF THE TERMS t1, t2, t3, t4
AND fn\n\
USED IN THE PROGRAM.\n\n");
if(r1=='2')

```

```

{
    printf("\nA FILE NAMED data1.in HAS BEEN GENERATED BY THIS
PROGRAM FOR ENTERING\n\ DATA IN THE DESIRED FORMAT.\n
    \nEnter\n\t\'1\' \tIF WANT TO EXIT THE PROGRAM AND\n\t
    \tEDIT THE ABOVE DATA FILE FOR ENTERING DATA.\n\n\t\'2\'
    \tIF\ YOU HAVE ALREADY EDITED THE INPUT DATAFILE AND\n
    \t\tARE READY FOR RUNNING THE PROGRAM\n\n ? ");
scanf("%c",&r2);
scanf("%c",&dummy);
if(r2=='2')
{
/*system("cp d.in data1.in"); */
    printf("\nEnter THE NO. OF THE SETS OF DATA : ");
    scanf("%d",&ns);
    scanf("%c",&dummy);
    ptdat1 = fopen(data1,"r");
    printf("\n\nWAIT ! \n\nSOLVING DIFFERENTIAL EQUATION !\n\n");
    for(i=0;i<ns;i++)
    {
        n=i;
        fscanf(ptdat1,"%g%g%g%g",&sigmax,&ylst,&h,&tmax);
        solve1();
    }
    fclose(ptdat1);
}
}
if(r2=='1')
{
    system("rm -f d.in");
    exit(-1);
}
if(r1=='1')
{
n=0;
do
{
    printf("\n\nEnter SIGMA, DIMENSIONLESS REACTION MODULOUS : ");
    scanf("%f",&sigmax);
    scanf("%c",&dummy);

    printf("\n\nEnter YL*, DIMENSIONLESS DISTANCE : ");
    scanf("%f",&ylst);
    scanf("%c",&dummy);
    printf("\n\nEnter h, STEP INCREMENT IN THE INDEPENDENT VARIABLE
TIME : ");
    scanf("%f",&h);
    scanf("%c",&dummy);
    (" \n\nEnter THE MAXIMUM VALUE OF THE INDEPENDENT VARIABLE UPTO
    \nWHICH DIFF. EQ. IS TO BE INTEGRATED : ");
    scanf("%g",&tmax);
    scanf("%c",&dummy);

```

```

scanf("%f",&tmin);
scanf("%c",&dummy);
printf("\n\nTHE DEPENDENT VARIABLE : ");
scanf("%f",&xin);
scanf("%c",&dummy);  */
solve1();
printf("\nDO YOU WANT TO ENTER ANOTHER SET OF DATA ? (y/n) : ");
scanf("%c",&r1);
scanf("%c",&dummy);
if(r1=='y') ++n;
ns=n+1;
} while (r1=='y');
}
}

```

```

/*****/

```

```

void solve1()
{
    ptdataout[n] = fopen(filename[n].fnd,"w");
    pttextout2[n] = fopen(filename[n].fnt2,"w");
    /*fprintf(ptdataout[n],"sigmax=%f\nylst=%f\n\n",sigmax,ylst);*/
    pttextout1[n] = fopen(filename[n].fnt1,"w");
    fprintf(pttextout1[n],"*****\n");
    fprintf(pttextout1[n],"sigmax=%f\nylst=%f\n\n",sigmax,ylst);
    fprintf(pttextout1[n],"\\tt1\\t\\tt2\\t\\tt3\\t\\tt4\\t    fn\\n");
    fprintf(pttextout1[n],"*****\n\n");
    tsti=tmin;
    x=xin;
    beta=be1(x);
    psi=exp(-beta * ylst);
    fprintf(ptdataout[n],"%f\\t%f\\n",tsti,psi);
    fprintf(pttextout2[n],"%f\\t%f\\n",tsti,x);
    j = 1;
    do
    {
        tsti=tmin+h*j++;
        xi=x;
        rk0 = h * fn1(tsti,xi);
        if((xi+0.5*rk0)>=0.999)
            break;
        rk1 = h * fn1(tsti+0.5*h,xi+0.5*rk0);
        if((xi+0.5*rk1)>=0.999)
            break;
        rk2 = h * fn1(tsti+0.5*h,xi+0.5*rk1);
        if((xi+rk2)>=0.999)
            break;
        rk3 = h * fn1(tsti+h,xi+rk2);
        x = xi+(rk0+2.*rk1+2.*rk2+rk3)/6.;
        if(xi>=0.999)
            break;
    }
}

```

```

        beta=be1(x);
        psi=exp(-beta * ylst);
        fprintf(pttextout2[n], "%f\t%f\n", tsti, x);
        fprintf(ptdataout[n], "%f\t%f\n", tsti, psi);
    } while((tsti<=tmax) && (x<=0.9999));
    fclose(ptdataout[n]);
    fclose(pttextout1[n]);
}

/*****/

float fn1(a1,a2)
float a1,a2;
{
    float a3;
    float be1();
    beta = be1(a2);
    a3 = beta * exp(-beta * ylst) + a1*0.0;
    return(a3);
}

/*****/

float be1(a)
float a;
{
    float a1;
    sigmaxsq1 = sigmax * sigmax;
    t1 = pow((1.-a), -1./3.);
    t2 = log(sigmax)/1.08;
    t3 = t2*t2;
    t4 = exp(-0.9*t3);
    a1 = 1./(1./3.*t1*t1+2.*sigmaxsq1*(t1-1.)+(0.21-0.62*a)*(1.+
        sigmaxsq1)*t4);
    fprintf(pttextout1[n], "\n    %f\t%f\t%f\t%f\t%f", t1, t2, t3, t4, a1);
    return(a1);
}

/*****/

```

# Appendix B

## Sample Simulations

Table B.1 gives the simulations for different assumed values of dimensionless reaction modulus,  $\sigma$  keeping dimensionless distance constant ( $y_L^* = 1$ )

Table B.2 gives the simulations for different assumed values of dimensionless distance,  $y_L^*$  keeping dimensionless reaction modulus constant ( $\sigma = 1$ )

Table B.1: Simulations for different assumed values of ' $\sigma$ ' ( $y_L^* = 1$ )

$t^*$	Dimensionless outlet conc. for different values of ' $\sigma$ '								
	0.2	0.4	0.8	1.2	1.6	2.0	3.0	6.0	10.0
0.0	0.064	0.114	0.222	0.301	0.354	0.389	0.423	0.363	0.234
0.1	0.065	0.114	0.217	0.297	0.356	0.399	0.464	0.571	0.698
0.2	0.067	0.113	0.212	0.294	0.359	0.411	0.502	0.669	0.791
0.3	0.068	0.113	0.208	0.292	0.364	0.424	0.537	0.725	0.833
0.4	0.070	0.113	0.205	0.291	0.370	0.439	0.569	0.762	0.858
0.5	0.072	0.113	0.202	0.292	0.378	0.455	0.597	0.789	0.874
0.6	0.074	0.114	0.200	0.294	0.388	0.472	0.623	0.809	0.886
0.7	0.076	0.115	0.199	0.298	0.400	0.491	0.646	0.824	0.896
0.8	0.078	0.116	0.199	0.303	0.414	0.510	0.667	0.837	0.903
0.9	0.081	0.117	0.200	0.311	0.430	0.529	0.686	0.848	0.909
1.0	0.083	0.119	0.202	0.321	0.447	0.550	0.704	0.857	0.915
1.1	0.086	0.121	0.206	0.333	0.466	0.570	0.720	0.865	0.919
1.2	0.089	0.123	0.211	0.348	0.487	0.590	0.734	0.872	0.923
1.3	0.093	0.126	0.218	0.366	0.508	0.610	0.748	0.878	0.926
1.4	0.097	0.130	0.227	0.387	0.531	0.629	0.760	0.883	0.930
1.5	0.101	0.134	0.238	0.410	0.554	0.648	0.771	0.888	0.932
1.6	0.105	0.139	0.252	0.436	0.578	0.666	0.782	0.892	0.935
1.7	0.111	0.145	0.269	0.465	0.602	0.684	0.792	0.896	0.937
1.8	0.116	0.152	0.291	0.496	0.626	0.701	0.801	0.900	0.939
1.9	0.123	0.160	0.316	0.528	0.649	0.717	0.809	0.903	0.941
2.0	0.130	0.170	0.346	0.562	0.671	0.733	0.817	0.906	0.943
2.1	0.138	0.182	0.381	0.596	0.693	0.747	0.824	0.909	0.944
2.2	0.147	0.195	0.421	0.629	0.714	0.761	0.831	0.912	0.946
2.3	0.157	0.212	0.467	0.663	0.734	0.774	0.838	0.914	0.947
2.4	0.169	0.232	0.516	0.695	0.753	0.787	0.844	0.917	0.948
2.5	0.182	0.257	0.568	0.726	0.771	0.798	0.850	0.919	0.950
2.6	0.198	0.286	0.623	0.756	0.788	0.810	0.855	0.921	0.951
2.7	0.216	0.322	0.677	0.783	0.804	0.820	0.860	0.923	0.952
2.8	0.238	0.365	0.731	0.810	0.819	0.830	0.865	0.925	0.953
2.9	0.263	0.417	0.782	0.834	0.833	0.839	0.870	0.927	0.954
3.0	0.293	0.479	0.831	0.857	0.847	0.848	0.874	0.928	0.955
3.1	0.330	0.550	0.877	0.879	0.860	0.857	0.878	0.930	0.956
3.2	0.373	0.629	0.919	0.900	0.872	0.865	0.882	0.931	0.956
3.3	0.426	0.715	0.956	0.919	0.883	0.872	0.886	0.933	0.957
3.4	0.489	0.802	0.000	0.937	0.894	0.880	0.890	0.934	0.958
3.5	0.564	0.884	0.000	0.954	0.904	0.887	0.893	0.935	0.959
3.6	0.651	0.952	0.000	0.971	0.914	0.893	0.897	0.937	0.959



Table B.2: Simulations for different assumed values of ' $y_L^*$ ', ( $\sigma = 1$ )

Dimensionless Time, $t^*$	Dimensionless outlet conc. for different values of ' $y_L^*$ '					
	0.2	0.4	0.8	1.2	1.6	2.0
0.000	0.767	0.588	0.346	0.203	0.120	0.070
0.100	0.759	0.578	0.339	0.200	0.118	0.070
0.200	0.755	0.572	0.333	0.196	0.116	0.069
0.300	0.759	0.571	0.328	0.193	0.114	0.068
0.400	0.772	0.577	0.326	0.191	0.113	0.067
0.500	0.793	0.592	0.326	0.189	0.112	0.067
0.600	0.819	0.614	0.328	0.187	0.111	0.066
0.700	0.846	0.644	0.336	0.186	0.110	0.065
0.800	0.872	0.679	0.342	0.186	0.109	0.065
0.900	0.894	0.717	0.354	0.186	0.108	0.064
1.000	0.913	0.755	0.371	0.187	0.107	0.064
1.100	0.929	0.790	0.392	0.189	0.107	0.063
1.200	0.943	0.823	0.417	0.192	0.106	0.063
1.300	0.954	0.852	0.447	0.196	0.106	0.063
1.400	0.964	0.877	0.482	0.201	0.106	0.062
1.500	0.972	0.899	0.520	0.207	0.106	0.062
1.600	0.980	0.918	0.560	0.214	0.107	0.062
1.700	0.986	0.935	0.603	0.223	0.107	0.061
1.800	0.991	0.950	0.645	0.234	0.108	0.061
1.900		0.963	0.687	0.247	0.109	0.061
2.000		0.975	0.727	0.262	0.110	0.061
2.100		0.986	0.765	0.280	0.111	0.061
2.200			0.800	0.300	0.113	0.061
2.300			0.833	0.323	0.115	0.061
2.400			0.863	0.350	0.117	0.061
2.500			0.891	0.380	0.119	0.061
2.600			0.916	0.413	0.122	0.061
2.700			0.939	0.448	0.126	0.061
2.800			0.961	0.487	0.130	0.061
2.900			0.980	0.527	0.134	0.061
3.000				0.569	0.139	0.061
3.100				0.612	0.144	0.062
3.200				0.654	0.151	0.062
3.300				0.696	0.158	0.062
3.400				0.737	0.166	0.063
3.500				0.776	0.176	0.063
3.600				0.814	0.186	0.064

# Appendix C

## Data Used for Simulation

*Source* : All the data given here have been taken from a Ph.D. thesis (Bhaskar, 1994).

### C.1 Data for active sodium carbonate

Length of the packed bed ( $L$ )	= 5.0 cm
Radius of the pellet ( $R_o$ )	= 0.635 cm
Molar density of the solid reactant ( $\rho_p$ )	= 0.0239 g-mole/ $cm^3$
Grain shape factor ( $F_g$ )	= 3
Void fraction of the bed ( $\epsilon_v$ )	= 0.42
Space velocity ( $U$ )	= 900 $hr^{-1}$
Fraction of reactive solids by weight ( $\omega$ )	= $\frac{1}{40}$

Table C.1: Data related to the active  $Na_2CO_3$  pellet

Decompn Temp., T K	Pore volume, $v_g$ ( $cm^3/g$ )	Porosity, $\epsilon_p$	Grain surface Area, $A_g$ ( $m^2/g$ )	Fractional vol. of sorbent in the bed
423	0.49	0.55	3.14	0.057
473	0.47	0.54	2.70	0.056
523	0.45	0.53	2.50	0.055
573	0.40	0.50	2.20	0.051
623	0.20	0.34	0.91	0.039

Variation of rate constant with temperature

$$k = A' e^{-\frac{E_a}{RT}} \quad (C.1)$$

where,

$$\begin{aligned} A' &= \text{Frequency factor} &= 0.022 \text{ cm/s} \\ k_a &= \text{Activation energy} &= 4224 \text{ cal/g-mole} \end{aligned}$$

Variation of effective diffusivity with temperature

$$D_e = 1.76 \times 10^{-11} T^{3.3} \quad (C.2)$$

**C.2 Data for calcined magnesium carbonate**

Length of the packed bed ( $L$ )	= 5 cm
Radius of the pellet ( $R_o$ )	= 0.075 cm
Molar density of the solid reactant ( $\rho_p$ )	= 0.0305 g-mole/ $cm^3$
Grain shape factor ( $F_g$ )	= 3
Void fraction of the bed ( $\epsilon_v$ )	= 0.42
Space velocity ( $U$ )	= 600 $hr^{-1}$
Fraction of reactive solids by weight ( $\omega$ )	= $\frac{1}{40}$

Table C.2: Data related to the calcined  $MgCO_3$  pellet  
(Calcination temp. = 750 °C)

Pore volume, $v_g$  ( $cm^3/g$ )	Porosity, $\epsilon_p$	Grain surface Area, $A_g$  ( $m^2/g$ )	Fractional vol. of sorbent in the packed bed
1.25	0.82	11.30	0.141

Variation of rate constant with temperature

$$k = A' e^{-\frac{E_a}{RT}} \quad (C.3)$$

where,

$$\begin{aligned} A' &= \text{Frequency factor} &= 7.12 \times 10^{-3} \text{ cm/s} \\ k_a &= \text{Activation energy} &= 8213 \text{ cal/g-mole} \end{aligned}$$

Variation of effective diffusivity with temperature

$$D_e = 1 \times 10^{-45} T^{13.4} \quad (C.4)$$

# Appendix D

## Simulated and Experimental Results

*Source* : All the experimental data given here have been taken from a Ph.D. thesis (Bhaskar, 1994).

## D.1 For sulphation of active sodium carbonate

Sulphation at different temperatures and an inlet conc. of 6000 ppm

Table D.1:  $T = 150^\circ C$

Dimensionless Time $t^*$	Dimensionless Outlet Conc.	
	Experimental	Predicted $\sigma = 14.4, y_L^* = 0.19$
0.006	0.157	0.384
0.011	0.462	0.512
0.022	0.678	0.640
0.033	0.791	0.706
0.045	0.820	0.747
0.056	0.873	0.778
0.067	0.888	0.798
0.083	0.876	0.820
0.100	0.812	0.837
0.117	0.885	0.850
0.134	0.885	0.861
0.150	0.888	0.869
0.167	0.906	0.877
0.184	0.864	0.883
0.200	0.892	0.888

Table D.2:  $T = 200^\circ C$ 

Dimensionless Time	Dimensionless Outlet Conc.	
	Experimental	Predicted $\sigma = 15.4, y_L^* = 0.28$
0.009	0.131	0.221
0.017	0.426	0.369
0.034	0.626	0.549
0.051	0.683	0.641
0.068	0.747	0.696
0.085	0.753	0.733
0.102	0.730	0.759
0.127	0.753	0.788
0.153	0.761	0.809
0.178	0.822	0.825
0.204	0.788	0.838
0.229	0.788	0.848
0.255	0.805	0.857
0.280	0.813	0.864
0.306	0.826	0.871

Table D.3:  $T = 250^\circ C$ 

Dimensionless Time	Dimensionless Outlet Conc.	
	Experimental	Predicted $\sigma = 15.6, y_L^* = 0.42$
0.013	0.103	0.058
0.025	0.153	0.123
0.051	0.361	0.331
0.076	0.465	0.481
0.101	0.572	0.573
0.126	0.634	0.633
0.152	0.685	0.676
0.189	0.712	0.719
0.227	0.685	0.750
0.265	0.715	0.774
0.303	0.754	0.792
0.341	0.768	0.806
0.379	0.805	0.818
0.417	0.826	0.828
0.455	0.838	0.837



Table D.4:  $T = 300^\circ C$ 

Dimensionless Time	Dimensionless Outlet Conc.	
	Experimental	Predicted $\sigma = 16.4, y_L^* = 0.59$
0.018	0.040	0.003
0.036	0.122	0.004
0.071	0.282	0.008
0.107	0.458	0.018
0.142	0.407	0.052
0.178	0.504	0.144
0.213	0.496	0.276
0.267	0.606	0.445
0.320	0.648	0.548
0.374	0.680	0.616
0.427	0.689	0.662
0.480	0.712	0.696
0.534	0.757	0.723
0.587	0.803	0.743
0.640	0.821	0.760

Table D.5:  $T = 350^\circ C$ 

Dimensionless Time	Dimensionless Outlet Conc.	
	Experimental	Predicted $\sigma = 17.4, y_L^* = 0.66$
0.020	0.241	0.0005
0.040	0.415	0.0005
0.079	0.612	0.0006
0.119	0.687	0.0007
0.159	0.747	0.0008
0.198	0.747	0.0010
0.238	0.756	0.0012
0.297	0.775	0.0018
0.357	0.834	0.0030
0.416	0.839	0.0059
0.476	0.820	0.0151
0.535	0.855	0.0513
0.595	0.865	0.1693
0.654	0.912	0.3293
0.714	0.934	0.4548

Sulphation of active sodium carbonate at different concentrations (  $T = 200\text{ }^{\circ}\text{C}$  ) :

Table D.6: Sulphation at different concentrations

Time (min)	Dimensionless Outlet Conc.							
	1500 ppm		3500 ppm		6000 ppm		18000 ppm	
	Expl.	Pred. $t^*1$	Expl.	Pred. $t^*2$	Expl.	Pred. $t^*3$	Expl.	Pred. $t^*4$
5	0.015	0.104	0.103	0.184	0.123	0.283	0.612	0.579
10	0.092	0.152	0.426	0.317	0.453	0.467	0.863	0.721
20	0.233	0.286	0.626	0.512	0.740	0.643	0.910	0.813
30	0.358	0.388	0.683	0.614	0.880	0.719	0.958	0.852
40	0.417	0.467	0.747	0.675	0.953	0.764	0.952	0.874
50	0.417	0.527	0.753	0.715	0.941	0.792	0.943	0.888
60	0.512	0.579	0.730	0.744	0.956	0.813	0.964	0.899
75	0.501	0.631	0.753	0.775	0.976	0.836	0.960	0.911
90	0.565	0.666	0.761	0.798	0.945	0.852	0.976	0.920
105	0.611	0.696	0.822	0.815	0.964	0.864	0.940	0.926
120	0.678	0.719	0.788	0.829	0.942	0.874	0.990	0.931
135	0.717	0.738	0.788	0.840	0.969	0.882	0.965	0.936
150	0.717	0.754	0.805	0.849	0.901	0.888	0.971	0.939
165	0.724	0.768	.813	0.857	0.957	0.894	0.982	0.942
180	0.748	0.779	0.826	0.864	0.961	0.900	0.974	0.945

For predicted data,

$$\sigma = 15.4, y_L^* = 0.27$$

$$t^* 1 = 1.212 \times 10^{-5} t$$

$$t^* 2 = 2.827 \times 10^{-5} t$$

$$t^* 3 = 4.846 \times 10^{-5} t$$

$$t^* 4 = 14.539 \times 10^{-5} t$$

## D.2 For sulphation of calcined magnesium carbonate

Sulphation at different temperatures (Conc. = 9000 ppm ).

Table D.7: T = 650 °C

Dimensionless Time	Dimensionless Outlet Conc.	
	Experimental	Predicted $\sigma = 11.5, y_L^* = 0.15$
0.0036	0.463	0.327
0.0072	0.608	0.379
0.0145	0.731	0.474
0.0217	0.731	0.550
0.0233	0.839	0.558
0.043	0.796	0.664
0.054	0.822	0.700
0.065	0.816	0.727
0.076	0.821	0.748
0.087	0.850	0.765
0.098	0.826	0.779
0.109	0.864	0.791
0.119	0.855	0.801
0.13	0.889	0.810

Table D.8:  $T = 750^{\circ}C$ 

Dimensionless Time	Dimensionless Outlet Conc.	
	Experimental	Predicted $\sigma = 7.5, y_L^* = 0.24$
0.0056	0.233	0.238
0.011	0.250	0.269
0.022	0.427	0.333
0.034	0.486	0.394
0.051	0.545	0.464
0.067	0.567	0.517
0.084	0.578	0.561
0.101	0.629	0.596
0.118	0.638	0.625
0.135	0.616	0.650
0.168	0.722	0.687
0.202	0.773	0.716

Table D.9:  $T = 850^{\circ}C$ 

Dimensionless Time	Dimensionless Outlet Conc.	
	Experimental	Predicted $\sigma = 5.2, y_L^* = 0.49$
0.012	0.246	0.194
0.024	0.336	0.209
0.047	0.471	0.239
0.071	0.537	0.270
0.106	0.604	0.314
0.141	0.604	0.355
0.212	0.648	0.428
0.247	0.655	0.459
0.283	0.688	0.487
0.318	0.715	0.512
0.353	0.704	0.534
0.389	0.808	0.555
0.424	0.814	0.573

Sulphation at different concentrations (  $T = 750^{\circ}\text{C}$  )Table D.10: Sulphation at different concentrations (  $T = 750^{\circ}\text{C}$  )

Time (min)	Dimensionless Outlet Conc.					
	2000 ppm		9000 ppm		22000 ppm	
	Expl.	Predicted $t^*1$	Expl.	Predicted $t^*2$	Expl.	Predicted $t^*3$
5	0.054	0.217	0.233	0.243	0.412	0.361
10	0.129	0.227	0.250	0.288	0.583	0.460
20	0.136	0.245	0.427	0.370	0.728	0.583
30	0.168	0.265	0.486	0.438	0.796	0.654
45	0.198	0.291	0.545	0.514	0.781	0.718
60	0.249	0.318	0.567	0.571	0.837	0.757
75	0.275	0.343	0.578	0.614	0.813	0.785
90	0.295	0.366	0.629	0.647	0.826	0.805
105	0.371	0.389	0.638	0.673	0.852	0.820
120	0.371	0.410	0.616	0.695	0.881	0.833
135	0.420	0.429	—	0.714	0.891	0.843
150	0.450	0.448	0.722	0.729	0.899	0.852
165	0.491	0.465	—	0.742	0.906	0.859
180	0.491	0.481	0.773	0.754	0.917	0.866

For predicted data,

$$\sigma = 7.5, y_L^* = 0.24$$

$$t^* 1 = 0.694 \times 10^{-5} \text{ t}$$

$$t^* 2 = 3.125 \times 10^{-5} \text{ t}$$

$$t^* 3 = 7.638 \times 10^{-5} \text{ t}$$